PERGAMON

Deep-Sea Research II 49 (2002) 2619–2648

DEEP-SEA RESEARCH
PART II

www.elsevier.com/locate/dsr2

Biogeochemical controls on new production in the tropical Pacific

Anthony K. Aufdenkampe[a,*], James J. McCarthy[c], Claudie Navarette[b], Martine Rodier[d], John Dunne[a], James W. Murray[a]

[a] *School of Oceanography, University of Washington, Box 355351, Seattle, WA 98195-5351, USA*
[b] *Université Paris VI, Paris, France*
[c] *Harvard University, Cambridge, MA, USA*
[d] *IRD, Station Marine d'Endoume, Marseille, France*

Received 20 July 2000; received in revised form 23 August 2001; accepted 20 September 2001

Abstract

Sources of variability in new production (NP) measured during nine cruises in the tropical Pacific Ocean are examined with respect to other biological and chemical properties. NP measured along the equator during the Zonal Flux and Flupac cruises using $^{15}NO_3$ incubation methods is presented in this paper and compared to similar data from seven previously published cruises to the tropical Pacific. The Zonal Flux cruise found a strong zonal gradient of increasing NP to the east that followed increasing nitrate inventories. NP values ranged from 0.8 and 3.8 mmol $N\,m^{-2}\,d^{-1}$ from 165°E to 150°W, respectively. During the 7-day Flupac Time Series II at 150°W, NP measurements also showed strong variability, ranging from 1.9 to 3.6 mmol $N\,m^{-2}\,d^{-1}$, despite relatively uniform nitrate. Both cruises observed a previously measured but seldom discussed trend for f-ratios to increase substantially at the limits of the euphotic zone (0.1% E_0).

Multiple linear regression (MLR) analyses of areal, depth-integrated data from 121 stations in the tropical Pacific previously have showed that variability in primary production (or chlorophyll), ammonium, nitrate and temperature together could "explain" 79% of the variability in NP (Aufdenkampe et al., Global Biogeochem. Cycles 15 (2001) 101). In the present study, the MLR method was extended to depth specific data, where the same variables were shown to explain 77% of nitrate uptake variability. MLR was then used to investigate differences between individual cruises in the relationships of NP to these variables. Similar to MLR results with combined data from all cruises, MLR of individual cruises also found primary production (or chlorophyll), ammonium and nitrate to be consistently the best variables to explain variability in areal NP, exhibiting R^2 values from 0.45 to 0.92. However, nitrate is consistently a much stronger predictor of NP within cruises than between cruises. Other lines of evidence—including plots of each property vs. NP and vs. standard residuals of the all-cruise MLR, and differences in MLR partial slopes for individual cruises—together demonstrate that the relationship of NP to nitrate exhibits subtle but real differences from one cruise to the next. Zonal Flux and Flupac sampled the two extremes of this observed NP-to-nitrate variability.

*Corresponding author. Now at: Stroud Water Research Center, 970 Spencer Road, Avondale, PA 19311, USA. Tel.: +1-610-268-2153; fax: +1-610-268-0490.

E-mail address: aufdenkampe@stroudcenter.org (A.K. Aufdenkampe).

0967-0645/02/$ - see front matter
PII: S0967-0645(02)00051-6

1. Introduction

Processes controlling primary production stimulated by newly available nutrients drive major biological links and feedbacks between oceanic carbon reservoirs and climate (Falkowski et al., 1998). Such new production (NP) (Dugdale and Goering, 1967) supports the biological pump of organic carbon export to the deep ocean (Eppley and Peterson, 1979), and the efficiency with which upwelled nutrients and dissolved carbon dioxide are sequestered by phytoplankton regulates carbon dioxide exchange with the atmosphere (Dugdale et al., 1992; Kurz and Maier-Reimer, 1993). For these reasons, the equatorial Pacific upwelling zone and other high-nitrate, low-chlorophyll (HNLC) regions have held the attention of the oceanographic community over the last decade (Murray et al., 1994; Barber et al., 1996; Feely et al., 1997).

While classically defined as "all primary production associated with newly available nitrogen" in the form of upwelled nitrate (Dugdale and Goering, 1967), the broad definition of NP requires consideration of all fluxes of limiting nutrients into the euphotic zone. These can include vertical and horizontal advective inputs, estuarine fluxes, nitrogen fixation, and atmospheric deposition. The fraction of NP to total primary production (PP) is referred to as the *f*-ratio. When considering the classical definition of new production, *f*-ratios are commonly calculated in terms of new and regenerated nitrogen uptake or in terms of carbon uptake.

$$f = \frac{\text{new production}}{\text{new} + \text{regenerated production}} \cong \frac{\mathrm{NO_3^-}\ \text{uptake}}{(\mathrm{NO_3^-} + \mathrm{NH_4^+} + \mathrm{NO_2^-} + \text{DON})\ \text{uptake}} \cong \frac{^{15}\mathrm{NO_3^-}\ \text{uptake}}{^{14}\mathrm{CO_2}\ \text{uptake}} \times \left(\frac{\mathrm{C}}{\mathrm{N}}\right)_{\text{plankton}}. \quad (1)$$

A corollary to the concept of new production is that, given steady-state nutrient inventories in the euphotic zone, new nutrient uptake must balance nutrient export in the forms of dissolved and particulate organic matter (Eppley and Peterson, 1979). Thus, the net flux of the limiting nutrient into the euphotic zone ultimately controls new production, and new nutrient uptake rates should equal export rates of those nutrients as organic matter when integrated over similar time intervals (Murray et al., 1989).

Previous studies of new production in the central equatorial Pacific in a variety of conditions have all found low *f*-ratios, with a mean of 0.16 ± 0.08 (Dugdale et al., 1992; Peña et al., 1992; McCarthy et al., 1996; Navarette, 1998; Raimbault et al., 1999), indicating the importance of nutrient recycling in maintaining primary production. These results fit nicely into the emerging understanding of the equatorial HNLC ecosystem as one in which limiting concentrations of iron and intense microzooplankton grazing jointly control phytoplankton biomass and production (Martin et al., 1994; Price et al., 1994; Fitzwater et al., 1996; Landry et al., 1997; Loukos et al., 1997) and maintain relatively constant rates of chlorophyll-specific primary production (P^B) (Barber and Chavez, 1991; Barber et al., 1996). However, variability in measured new production (0.03–6.2 mmol $\mathrm{N\,m^{-2}\,d^{-1}}$) is an order of magnitude greater than that of primary production (5–180 mmol $\mathrm{C\,m^{-2}\,d^{-1}}$) and the range of *f*-ratios observed in the region, 0.01–0.46, is substantial (Aufdenkampe et al., 2001). The recent appreciation of such strong variability in new production contrasts the earlier paradigm of a biologically stable tropical Pacific ecosystem. Clearly, the biogeochemical and physical controls on new production cannot be identical to those for primary production.

Attempts to explain the variability of new production in the tropical Pacific by comparison with simple parameters has not proven to be straightforward. Previous studies have indeed shown some correlations between nitrate uptake rates vs. nitrate, ammonium, chlorophyll or diatom concentrations (Wheeler and Kokkinakis, 1990; Peña et al., 1992; McCarthy et al., 1996; Landry et al., 1997; Raimbault et al., 1999), yet no single relationship had remained robust from one cruise to another. However, recent multivariate statistical analysis of new production and related data from 121 stations in the tropical Pacific (Aufdenkampe et al., 2001) demonstrates that

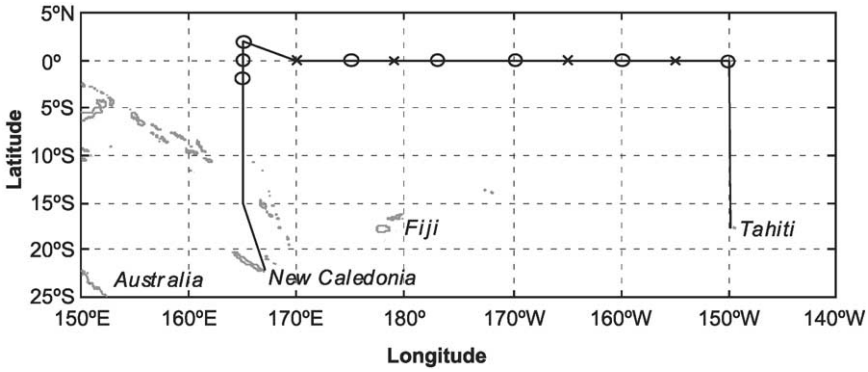

Fig. 1. Cruise track for both Zonal Flux and FluPac cruises. Stations occupied during Zonal Flux are marked by circles (24 h stations) and crosses (6–8 h stations).

variability in new production for the entire region is indeed related ($R^2 = 0.79$) to other properties (primary production (or chlorophyll), ammonium, nitrate and temperature), but only when all are considered simultaneously. These findings advance our ability to extrapolate new production estimates to finer spatial and temporal scales and refine our understanding of what controls new production. However, such statistical models do not directly address the primary controls on new production, which must be the fluxes of bioactive elements into the upper-ocean ecosystem.

A zonal transect along the equator in the Pacific Ocean is in many ways the ideal natural laboratory to study the consequences of varying fluxes of bioactive elements into the euphotic zone. Physical conditions—advective patterns, residence times, stratification, source waters, incident light, and euphotic zone depths—are all generally uniform throughout the upwelling zone, leading to relatively constant primary production, chlorophyll and other biological features (Barber and Chavez, 1991; Chavez et al., 1996; Le Borgne et al., 1999, 2002). Underlying these patterns, however, is the classic deepening of temperature and nutrient isolines from east to west (Barber and Kogelshatz, 1990), which results in a strong zonal gradient of upwelling nutrient fluxes to the surface. The general trend of increasing upwelling yet constant productivity offers the perfect opportunity to separate processes that control new vs. primary production. The Zonal Flux cruise in April 1996 sampled such a transect, from 165°E to 150°W (Fig. 1), during mild La Niña conditions in which the nutrient-depleted warm pool was pushed completely west of the study region (Fig. 2a) (Le Borgne et al., 1999). The France-JGOFS Flupac cruise sampled the same transect in October 1994, during moderate El Niño conditions (Eldin et al., 1997).

In this paper, we first present new production data from the Zonal Flux cruise and Flupac Time Series II (at 150°W), as determined by $^{15}NO_3$ uptake incubations. These data are used to explore measurement issues that are broadly applicable to all ^{15}N-based nitrate uptake studies—an investigation of day vs. night nitrate uptake rates, a comparison of on-deck vs. in situ incubation methods, and a detailed analysis of procedural and analytical uncertainties associated with $^{15}NO_3$-based new production estimates. The second objective of the paper is to examine trends in new production with respect to other chemical and biological properties. We build upon previous multivariate statistical analyses (Aufdenkampe et al., 2001) by comparing relationships observed during Zonal Flux and Flupac TS II to those observed during the previous meridional studies of new production at 140°W (McCarthy et al., 1996) and 150°W (Dugdale et al., 1992; Peña et al., 1992; Wilkerson and Dugdale, 1992; Raimbault et al., 1999), and the two time series on the equator at 140°W (Wheeler, 1995). We conclude by making the case that the Zonal Flux and Flupac cruises

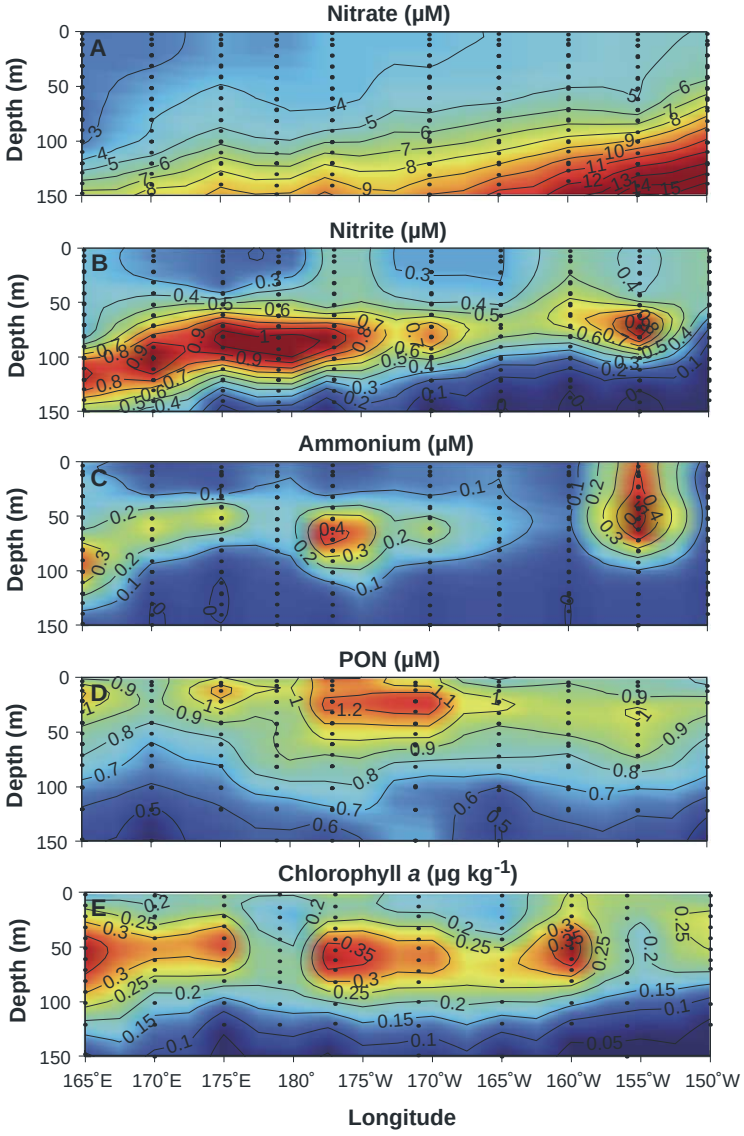

Fig. 2. Zonal Flux contours of (a) nitrate (μM), (b) nitrite (μM), (c) ammonium (μM), (d) suspended particulate organic nitrogen (μM), and (e) chlorophyll *a* (μg kg^{-1}) concentrations. Sampling locations are marked by black dots and may represent more than one collection cast. Contours are calculated by objective analysis of all nutrient data collected during the cruise.

sampled the extreme end-members of the processes that control new production in the region. In a companion paper (Aufdenkampe and Murray, 2002), the comparisons made here are used as a springboard to explore, with a simple euphotic zone box model of nitrogen and iron fluxes, the role of iron and physical forcing in controlling the relationship of new production to nitrate.

2. Methods

2.1. Site description and sample collection for Zonal Flux and Flupac

The Zonal Flux cruise (R./V. *Thompson*, TTN-060) occupied twelve stations from April 15 to May 14, 1996 (Le Borgne et al., 1999)—ten along

the equator from 165°E to 150°W and two stations at 2°N and 2°S at 165°E (Fig. 1). Eight stations were sampled intensively for over 24 h. These stations included deployment of sediment trap arrays and in situ primary and new production incubation arrays in addition to casts for nutrient, chlorophyll, bio-optic, bacteria, zooplankton, TOC, and suspended particulate samples. Hydrographic data were collected using a Sea-Bird SBE9 + CTD. Light-level depths—defined as the depth at which certain percentages of photosynthetically active radiation (PAR) are attenuated from incident surface radiation (E_0)—were measured as a component of optical casts with a SAtlantic OCP200 spectroradiometer coupled to a surface reference cell (courtesy of Scott Pegau, Oregon State University). At the four short stations no trap or incubation arrays were deployed.

The France-JGOFS Flupac cruise (R./V. *L'Atalante*) followed a similar cruise track as Zonal Flux from September 23 to October 28, 1994 (Le Borgne and Gesbert, 1995). Here, we focus on the second of two time series, at 150°W (October 19–25), for which new production was measured for seven consecutive days. Intensive sampling and biological measurements were made throughout the time series, similar to the 24-h stations of Zonal Flux. Hydrographic data were collected using a Sea-Bird SBE-911 CTD.

2.2. In situ and on-deck nitrate uptake incubations during Zonal Flux

At each of the 12 stations, water was collected from a 24 Niskin bottle General Oceanic rosette 1–2 h prior to sunrise at seven depths. These depths were chosen to correspond to levels of 50%, 30%, 14%, 8%, 5%, 1%, and 0.1% E_0, which were estimated from the previous station's optical casts. Water was carefully transferred from the Niskin to 1.2-l polycarbonate bottles with silicon rubber tubing to prevent turbulent disturbance of organisms and immediately placed in a dark bag. Incubations were initiated by addition of ^{15}N labeled nitrate (98 at%) corresponding to 10% of the ambient concentration in each bottle, as estimated from the previous day's nutrient casts. A single, refrigerated $K^{15}NO_3$ stock was used throughout the cruise, and repeated nitrate analyses confirmed no drift in the stock concentration. All bottles and tubing were cleaned with 1 N HCl and then rinsed with nanopure water (Barnstead) and three times with sample water.

Bottles for in situ incubations were tied to the kevlar line of the primary productivity array at levels corresponding to their collection depths. The array and floats were then deployed from the ship for an average of 6.5 h (ranging from 5.2 to 7.8 h, with 6 of 8 between 6.0 and 7.0 h). Incubations lasted an average of 8.2 h (ranging from 6.4 to 9.7 h, with 6 of 8 between 7.1 and 9.0 h) and were terminated by filtration onto pre-combusted (2 h at 450°C) Whatman® GF/F filters.

Bottles for on-deck incubations were individually placed in light attenuators, which were composed of nesting light and dark blue Plexiglas boxes and bags of neutral density screening. Just before sunrise, the bagged and boxed bottles were placed in a large bath on the ship's fantail that was irrigated with sea-surface water to prevent solar heating. The light-attenuation boxes were calibrated on the fantail during a cloudless day by inserting the spherical probe of a Biospherical Instruments QSL-100 quantum scalar irradiance meter into an empty bottle, which was then placed within combinations of Plexiglas boxes and screening. The incubators transmitted the following percentages of E_0: 51.1%, 32.8%, 16.8%, 7.6%, 4.4%, 0.71%, 0.10%. Deployment lasted an average of 5.4 h (range of 4.5–6.8, with 10 of 12 between 4.8 and 6.2) and incubations an average of 6.4 h (range of 5.5–9.5, with 10 of 12 between 5.7 and 7.1). Time-series sampling over similar incubations periods on previous cruises confirmed that complications due to growth, grazing and potential depletion of nutrients were minimal (McCarthy et al., 1996). In addition, by being longer than 2–4 h, incubations minimized effects of "surge" uptake at dawn, thus offering less biased extrapolation of uptake rates to the afternoon. Lastly, duration of incubations were highly uncorrelated with uptake rates for Zonal Flux.

Four incubations also were conducted at night, using water collected near midnight from the same depths as that day's morning incubations. Bottles

were placed in the on-deck incubator, which was covered to exclude light completely. Night incubations averaged 5.5 h (range of 4.7–6.0).

At each station, one depth was chosen to run triplicate incubation bottles for in situ, on-deck, and night-time incubations. Over the course of the cruise all depths were replicated at least once in this manner.

2.3. In situ nitrate uptake incubations during Flupac

Water was collected 1–2 h prior to sunrise from twelve depths between the surface and 150 m from a rosette equipped with experimental, trace-metal free, "Noex" (Technicap) bottles designed to eliminate contact with surface films. Collection into 2.3- or 4.6-l polycarbonate bottles, cleaned similarly to those during Zonal Flux, was performed in the dark. In situ incubations with $K^{15}NO_3$ (99 at%) were initiated, deployed, and terminated in a similar fashion as for Zonal Flux. Labeled nitrate additions were targeted to 10% of ambient concentrations. Incubations were deployed at the 12 collection depths on the in situ primary production array and were terminated by filtration onto pre-combusted GF/F filters. Half- and full-light day incubations were run at each station, lasting an average of 5.6 h (range of 5.3–5.8) and 11.9 h (range 11.4–12.9), respectively. Differences between the two sets of incubations were minimal. Thus, only data from the shorter incubations are presented here, for more direct comparison with data from Zonal Flux and most previous cruises. Due to collection problems with the Noex bottles, certain incubation bottles needed to be "discarded," leaving 5–8 depths for each profile. These pared profiles, while sparse below 60 m, are well sampled at surface depths where most nitrate uptake occurs. Therefore, minor reconstruction of some missing values with averages does not significantly degrade estimates of magnitude or variability between profiles. More details of these methods can be found in Navarette (1998).

Euphotic zone light-level depths were calculated from chlorophyll profiles using the optical model of Morel (1988, Matlab code courtesy of Z. Johnson and R.T. Barber, Duke University) and adjusted by the ratios of modeled to measured depths found during the Zonal Flux cruise, which averaged 0.85 ± 0.05 and 0.95 ± 0.15 for the 1.0% and 0.1% E_0 depths, respectively.

2.4. ^{15}N and PON analysis

For Zonal Flux, quantitative analysis of ^{15}N enrichment and particulate organic nitrogen (PON) concentration of the filtered samples were determined simultaneously on each filter with an Europa Scientific model 20/20 Mass Spectrometer equipped with an automated Dumas combustion sample preparation system (model ANCA nt) in a continuous flow configuration. The combustion column has been modified with a quartz tubing insert to limit complications due to sea salts and glass-fiber filter residues (McCarthy et al., 1999).

Isotopic analysis for Flupac samples were made with a SOPRA model GS1 Emission Spectrometer after combustion to N_2 as per the method of Guiraud and Fardeau (1980) and as described in Navarette (1998). PON was determined with a Perkin Elmer 2400 CHN Analyzer on a duplicate of each isotope sample, which also allowed for calculation of the N_2 partial pressure in the sample ampoule for each emission analysis.

2.5. Uptake rate calculations

Nitrate uptake rates, expressed as ρ or ρNO_3 ($nM\,h^{-1}$), were calculated using the method of Dugdale and Wilkerson (1986) by multiplying the measured specific uptake rate, V, by the corresponding PON. Depth integration of ρNO_3 over the euphotic zone for in situ profiles was performed by trapezoidal summation, with surface values assumed to equal those at the shallowest depth. For integration of Zonal Flux on-deck incubations it was necessary to assign a depth for each incubation bottle based on the actual PAR profile for that station. Because these depths were never the same depths where water was collected, calculations of ρNO_3 for the simulated depth required interpolation of PON to the correct depth. This correction assumes that V does not vary significantly over 5–10 m changes in collection depth. In addition, it was necessary to

interpolate ρNO_3 values to the exact 1.0% and 0.1% E_0 light-level depths for direct comparison between in situ, on-deck and previous values.

Daily new production values were calculated by the weighted sum of the morning and night uptake rates for each station ($NP = 12 \int \rho_{night} + 12 \int \rho_{day}$). The morning rates (6-h incubations) were extrapolated to the full solar day without correction, as is commonly done (Peña et al., 1992; Wilkerson and Dugdale, 1992). For Zonal Flux, night-time uptake rates for the eight stations with no direct measurements were estimated from linear regressions of the measured night-time rates as a function of their respective day time rates (presented in results). Night-time uptake during Flupac was calculated from these same equations. All new production rates presented in carbon units are calculated by multiplying nitrate uptake values by the molar Redfield C/N ratio of 6.6. Likewise, all *f*-ratios discussed in this paper are calculated according to the right side of Eq. (1) with C/N= 6.6.

2.6. Nutrients, chlorophyll, and primary production

Nutrient, chlorophyll, and routine PON concentrations and rates of primary production were all determined in parallel to new production measurements for both cruises, with samples being collected for all four analyses from the same cast at the same depths. Nutrients (NO_3, NO_2, NH_4, PO_4, $Si(OH)_4$) were analyzed immediately on board with a Technicon Autoanlayzer II for both cruises (Bonnet, 1995). The method of Grasshoff et al. (1983) was employed for NH_4 and the classical method of Strickland and Parsons (1972) for NO_3. A high-sensitivity method (Oudot and Montel, 1988) was used for NO_2 and for NO_3 below 1.0 μM. The lower limits of detection of the various analyses were: 0.003 μM for NO_3 and NO_2 (<1.0 μM), 0.02 μM for NO_3 (>1.0 μM), 0.02 μM for NH_4, 0.01 μM for PO_4, and 0.05 μM for $Si(OH)_4$. Difficulties with the ammonium method were encountered during Flupac; therefore, NH_4 data from this cruise should be considered to have larger unquantifiable uncertainties than the rest of the data. Chlorophyll *a* concentrations (Le Borgne et al., 1999) were analyzed on a Turner fluorometer after filtration onto GF/F filters and subsequent methanol extraction (courtesy of Aubert Le Bouteiller, IRD France), according to the method described by Le Bouteiller et al. (1992). Routine PON was collected by filtering 4 l of water from Niskin bottles onto pre-combusted Whatman® GF/F filters and analyzed on a Perkin Elmer 2400 CHN analyzer. Primary production was measured at 12 depths, from 0 to 150 m, by a ^{14}C method similar to Barber et al. (1996) for 12-h in situ incubations using the drifting array described above (courtesy of Aubert Le Bouteiller, IRD, France).

2.7. Uncertainty analysis of Zonal Flux new production estimates

In this paper, measured nitrate uptake rates are followed by their standard errors (SE) (calculated as described below) and means are followed by their corresponding standard deviations. The coefficient of variation (CV) is the standard error given as a percentage of the mean or calculated value.

For Zonal Flux results, average measurement uncertainties for each incubation were propagated through to the calculated nitrate uptake rates and depth-integrated new production via "Monte-Carlo" bootstrapping methods. For each of the six measured values required to calculate each nitrate uptake rate, 5000 normally distributed random numbers were generated, with a mean value corresponding to that measured and a standard deviation corresponding to the estimated or assumed uncertainty for the measurement. These values were then used to compute 5000 nitrate uptake rates, whose standard deviation was taken as the uncertainty estimate for the originally calculated nitrate uptake rate. Uncertainties in each depth-integrated new production value were estimated in the same way, by integrating the 5000 nitrate uptake profiles over their respective depths (which were also assumed to have uncertainties). For each station, these values were found to be normally distributed and consistently exhibited a mean that matched the originally calculated values to the third significant figure.

The following is a list of each measured term with its assumed uncertainty for this study:

- *Ambient Nitrate Concentration*. $\pm 0.06\,\mu M$, which was the variability in eight measurements over the course of the cruise of a preserved $2.0\,\mu M$ solution. Analytical precision on any single day was $\pm 0.01\,\mu M$.
- *$^{15}NO_3$ Concentration in Addition*. $\pm 2.2\%$ uncertainty in the stock addition due to dilution errors and stock concentration uncertainty.
- *At% ^{15}N in Addition*. ± 1 at% error is likely in the actual ^{15}N enrichment of the stock, given the difficulty in measuring enrichments as high as 98 at%.
- *Incubation Time*. ± 10 min, which is a rough estimate to indicate not only the imprecision of start and end times (perhaps ± 2 min each), but also the uncertainty inherent in the "dark" and "filtration" periods of the incubation.
- *At% ^{15}N of sample*. $\pm 1.42\%$. Mean of standard deviations of isotope measurements made on triplicate incubations during the study ($n = 23$), given as the CV. The range of CV's for individual triplicate sets was 0.29–5.99% (SD = $\pm 1.35\%$).
- *PON*. $\pm 4.46\%$. This is the mean of the standard deviations of [PON] measurements made for all triplicate incubations during the study ($n = 23$), given as the CV. The range of CV's for individual triplicate sets was 0.16–10.39% with a standard deviation of $\pm 2.52\%$. Uncertainty in PON is arbitrarily assumed to be 50% greater when interpolated to the depths simulated by on-deck incubations.
- *Incubation Depth*. 1 m for in situ incubations or increasing from 2 to 5 m with depth for on-deck incubations. The latter is roughly based on the variability observed in duplicate optical casts, but does not include uncertainties in the calibration of light conditions within the incubator (which are likely to be systematic, rather than random).

Sensitivity analysis was performed by doubling each of these uncertainties one at a time while keeping the others constant. The percent change in the uncertainty of both the ρNO_3 values and the depth-integrated new production values were then used as estimates of the sensitivity of final uncertainties to uncertainties in that particular measurement.

2.8. Statistical analyses

Multiple linear regression (MLR) methods used in this paper are identical to those employed in Aufdenkampe et al. (2001). MLR fits a hyperplane to multidimensional data, yielding a regression equation analogous to that of simple linear regression (Neter et al., 1996)

$$Y = \beta_0 + \beta_1 X_1 + \beta_2 X_2 + \cdots + \beta_n X_n, \tag{2}$$

where β_0 is the intercept and β_i the slope of the independent variable X_i (Neter et al., 1996). In this paper, values of β are followed by their SE. The adjusted multiple coefficient of determination, R^{2*}, is corrected for reductions in degrees of freedom as independent variables are added. Thus R^{2*}, unlike R^2, reaches a maximum with the best combination of the minimum number of independent variables, decreasing with subsequent variable addition. Subset methods of variable selection were used in this study to choose the set of independent variables that maximized R^{2*} (Neter et al., 1996). Partial correlation coefficients, such as $r_{Y3.12}$, indicate the relative contribution of each variable to the overall MLR fit and are analogous to the simple correlation coefficients presented in this paper based on Pearson's product-moment, except that the latter do not take into account issues of covariance (Sokal and Rohlf, 1995).

The nature of oceanic research is such that sample sizes are often too small for conclusive statistical interpretation. Therefore, throughout this paper, p-values are provided for all marginal statistics so that the reader can determine his/herself whether, for example, a 9% probability of being random is meaningful. Often, p-values for similar non-parametric statistics (such as Spearman rank correlation) also are given for comparison.

3. Results

3.1. Zonal Flux: chemical and biological properties

During the April 1996 La Niña event (Southern Oscillation Index, SOI = 0.6) sampled by the Zonal Flux cruise, the cold tongue of equatorial upwelling extended to 158°E (Le Borgne et al., 1999), displacing its boundary with the western warm pool over 20° westward from the climatological mean near 180° (Barber and Chavez, 1991). This strong upwelling condition corresponded in a gradual eastward shoaling of the 25° isotherm and the coinciding 7 μM nitrate isopleth from ~145 m at 165°E to ~60 m at 150°W (Fig. 2a) (Le Borgne et al., 1999). Temperature and nitrate profiles show a break in slope just above these isolines, from relatively constant near-surface values to an even gradient below. Mixed-layer depths, as defined by $\Delta\sigma_\theta = 0.125$ (Gardner et al., 1995) did not show a matching trend with longitude and were highly variable, even between casts at the same station, ranging from 32 to 94 m with a mean of 52 ± 15 m. Nitrite exhibited a very distinct maximum of 0.5–1.6 μM just at or just above the nitracline (Fig. 2b). This ~40-m-thick layer gradually shoaled eastward along with the nitracline. Ammonium concentrations varied more between stations (Fig. 2c) with a maximum at 20–30 m above the nitracline and nitrite maximum.

Despite the striking temperature and nutrient gradient, planktonic biomass—as estimated from euphotic zone inventories of chlorophyll *a* (Table 1, Fig. 2e) and also particulate organic phosphorus (POP), bacteria, and mesozooplankton—exhibited slight although significant decreases (Spearman rank correlation, $p < 0.05$) from west to east (Le Borgne et al., 1999). Le Borgne et al. (1999) point out, however, that the total range in these biomass values was quite similar to that observed during the 6-day Flupac Time Series II at 150°W (Table 1, Fig. 4d). In contrast, PON was variable and did not have a zonal trend (Fig. 2d). Measured euphotic zone depths, while varying around 76 ± 4 m for the 1.0% light level and 132 ± 9 m for the 0.1% light level, also exhibited no zonal trend (Table 1).

Le Borgne et al. (1999) showed that primary production exhibited no discernable zonal gradient yet ranged from 76 to 96 mmol C $m^{-2} d^{-1}$ when integrated to 0.1% E_0 depths (Table 1, Fig. 3c). These values fall near the center of the range measured during the six EqPac cruises at 1°S–1°N and 140°W (Barber et al., 1996). Chlorophyll-specific primary productivity (P^B) integrated to 0.1% E_0 was relatively constant at stations west of 170°E, with a mean of 41 ± 2 mg C mg^{-1} Chl^{-1} d^{-1}, but was significantly lower at 165°E, where values were 23 and 30 mg C mg^{-1} Chl^{-1} d^{-1} at 2°S and the equator, respectively. Particulate organic carbon fluxes, estimated both by drifting sediment traps (Le Borgne et al., 1999) and by ^{234}Th deficiency modeling (Dunne et al., 2000), gave values ranging from 7.3–17.1 and 7.8–12.6 mmol C $m^{-2} d^{-1}$, respectively, with a slight but not significant decreasing eastward trend for the former.

3.2. Zonal Flux: transect of new production at the equator

Contour plots of nitrate uptake rates, ρNO_3, show a general increase from west to east for both in situ and on-deck estimates (Fig. 3a and b), although this trend is not as uniform as the shoaling of the nutricline (Fig. 2a). Maximal in situ ρNO_3 ranged from 1.38 ± 0.14 nM h^{-1} at 165°E to 7.03 ± 0.45 nM h^{-1} at 150°W, corresponding to V_{NO_3} of 1.57 ± 0.14 and $8.33 \pm 0.37 \times 10^{-3}$ h^{-1}. Vertical distributions of ρNO_3 showed that greater than two-thirds of integrated new production occurred in the upper 40 m. Below 20 m uptake rates decreased steadily with depth, although minimum values of ρNO_3 occurred at the 1.0% I_0 levels rather than the 0.1% I_0 depths for all stations west of 165°W. These minimum values ranged from 0.037 ± 0.037 M h^{-1} at 165°E to 0.563 ± 0.061 nM h^{-1} at 170°W, corresponding to V_{NO_3} of 0.073 ± 0.073 and $1.33 \pm 0.13 \times 10^{-3}$ h^{-1}.

In situ incubations gave systematically higher estimates than corresponding on-deck incubations (Table 1, Fig. 3a and b), with the ratio of depth-integrated in situ to on-deck rates ranging from 1.15 to 1.99 (mean of 1.45 ± 0.29) for rates integrated to 1.0% E_0 and 1.19 to 1.63

Table 1
New production measured during the Zonal Flux and Flupac cruises

Station	Latitude	Longitude	Date (mm/dd/yy)	Depth of light levels (m)		On-deck New Production (mmol N $m^{-2} d^{-1}$)		In situ New Production[a] (mmol N $m^{-2} d^{-1}$)		In situ Primary Prod.[b] (mmol C $m^{-2} d^{-1}$)		In situ *f*-ratio[c] NP/PP[c]		$\int[NO_3^-]$ (mmol m^{-2})		$\int[NH_4^+]$ (mmol m^{-2})		$\int[Chl_a]$ (mg m^{-2})	
				1% E_0	0.1% E_0	1% E_0	0.1% E_0	1% E_0	0.1% E_0	1% E_0	0.1% E_0	1% E_0	0.1% E_0	1% E_0	0.1% E_0	1% E_0	0.1% E_0	1% E_0	0.1% E_0
Zonal Flux equatorial transect																			
1	2°S	165°E	4/20/96	85	146	0.43	0.61	0.77	0.90	51.5	55.5	0.099	0.107	158.1	391.1	15.55	40.13	20.26	28.67
6	2°N	165°E	4/24/96	69	126	1.64	1.93	2.05	2.34	94.8	99.4	0.142	0.155	144.5	325.2	4.67	5.89	21.41	29.38
3	0°	165°E	4/22/96	76	113	0.49	0.68	0.79	0.97	81.1	85.8	0.064	0.075	208.5	374.8	7.99	24.50	22.97	34.73
7	0°	170°E	4/26/96	77	133	1.36	1.64	(1.8)	(2.2)	(90)	(100)	(0.14)	(0.14)	235.9	484.4	15.08	20.41	20.66	29.02
8	0°	175°E	4/28/96	79	140	2.18	2.51	2.47	2.91	86.6	92.6	0.188	0.207	301.2	687.5	13.45	14.48	19.44	26.05
9	0°	180°	4/30/96	78	138	1.49	1.67	(2.0)	(2.2)	(75)	(90)	(0.18)	(0.16)	277.8	635.3	10.73	13.74	17.30	26.35
10	0°	177°W	4/31/96	76	135	1.47	1.73	2.12	2.42	83.1	89.6	0.169	0.179	296.7	716.1	19.38	21.65	20.37	27.64
11	0°	170.7°W	5/2/96	75	128	1.86	2.11	2.11	2.57	82.8	95.7	0.168	0.177	314.4	668.3	13.97	17.23	17.72	26.65
12	0°	165°W	5/4/96	75	133	1.98	2.43	(2.7)	(3.2)	(74)	(91)	(0.24)	(0.23)	323.5	765.8	9.64	11.83	17.03	26.36
13	0°	160°W	5/6/96	75	138	2.02	2.28	2.83	3.20	83.2	88.6	0.224	0.238	358.9	961.4	7.14	7.89	21.58	27.98
14	0°	155°W	5/8/96	73	131	1.12	1.31	(1.5)	(1.7)	(75)	(88)	(0.13)	(0.13)	355.0	825.5	32.50	42.21	17.31	25.54
15	0°	150°W	5/9-10/96	71	123	2.86	3.25	3.74	4.42	72.7	76.3	0.340	0.382	426.1	1010.4	4.65	5.06	16.10	20.85
Flupac Time Series II																			
1	0°	150°W	10/19/94	83	133	—	—	3.31	3.72	97.4	102.1	0.225	0.240	296.8	531.0	13.33	19.42	22.79	28.67
2	0°	150°W	10/20/94	83	129	—	—	3.83	4.16	103.7	108.9	0.244	0.252	284.0	490.4	7.35	16.24	23.84	30.94
3	0°	150°W	10/21/94	84	128	—	—	2.05	2.42	99.1	102.5	0.137	0.156	278.4	438.6	39.62	55.12	22.76	29.78
4	0°	150°W	10/22/94	81	129	—	—	2.45	2.81	100.8	105.7	0.161	0.176	292.3	526.3	7.81	9.24	22.77	27.86
5	0°	150°W	10/23/94	78	129	—	—	3.53	3.88	99.4	104.2	0.235	0.246	260.5	513.3	9.80	14.83	22.53	28.33
6	0°	150°W	10/24/94	80	124	—	—	2.88	3.26	100.2	107.5	0.190	0.200	258.5	498.1	9.00	16.02	20.92	28.05
7	0°	150°W	10/25/94	83	126	—	—	2.64	3.00	91.5	98.3	0.190	0.201	247.8	455.4	12.92	17.17	19.92	26.10

[a] In situ new production values in parentheses were estimated by multiplying new production measured on-deck by the cruise average in situ to on-deck ratio.
[b] Primary production values in parentheses were estimated by multiplying the station chlorophyll concentrations by the cruise average P^B west of 165°W.
[c] *f*-Ratios are calculated by the ratio of new to total primary production, where new production is converted to carbon units by multiplying by 6.6.

(1.40 ± 0.16) for 0.1% E_0 rates. Differences between in situ and on-deck incubation methods are typically attributed to poor assignment of light-level depths simulated by the on-deck incubators due to: (1) errors in the estimation of actual light-level depths at each station, and (2) differences in incident irradiance between the water's surface and on the deck of a ship (Barber et al., 1997). Because of confidence in bio-optical profiles during the cruise, it seems that configuration of the incubators somehow decreased incident light to the on-deck incubators through partial shading or differences in reflectance within the seawater bath relative to calibration conditions. As a result, only in situ nitrate uptake values are considered for the remainder of this paper. However, for the four stations in which no in situ measurements were made, daily depth-integrated new production was estimated as the on-deck value divided by the cruise average on-deck to in situ ratio.

Daily depth-integrated new production to 1.0% E_0 increased from 0.77 ± 0.06 mmol $N\,m^{-2}\,d^{-1}$ at 165°E to 3.74 ± 0.11 mmol $N\,m^{-2}\,d^{-1}$ at 150°W (Table 1), exhibiting a clear zonal trend ($p < 0.05$) even when including the on-deck incubation at 155°W. These values represent some of the highest and some of the lowest values measured in the tropical Pacific region (Aufdenkampe et al., 2001), although most previous measurements were made east of 150°W. However, during El Niño conditions in the western oligotrophic warm pool at 167°E, average new production measured during Flupac Time Series I was 1.3 mmol $N\,m^{-2}\,d^{-1}$ (Rodier and Le Borgne, 1997; Navarette, 1998).

As a consequence of the zonal uniformity in primary production, the *f*-ratio of new to total primary production increased from west to east in a similar pattern as new production (Table 1, Fig. 3c and d), with depth-integrated values to 1.0% E_0 ranging from 0.064 at 165°E to 0.34 at 150°W. The Redfield assumption ($C/N = 6.6$) used to convert new production to carbon units appeared reasonable, as the POC/N in drifting sediment traps equaled 6.77 ± 0.46 ($n = 24$) and showed no appreciable zonal trend. Contours of *f*-ratios (Fig. 3d) revealed interesting structure. The mid-euphotic zone (1–8% E_0 or 40–80 m) had very low *f*-ratios west of 165°W, ranging from 0.04 to 0.16, whereas shallower values were twice as high, perhaps hinting at the relative importance of atmospheric iron fluxes in this half of the transect. East of 165°W, *f*-ratios were uniform to 80 m depth. Most striking was the dramatic increase in *f*-ratio at the 0.1% I_0 depth for all stations, with values ranging from 0.38 to 6.5. At this highest *f*-ratio, the plankton community was taking up one mole of nitrate for each mole of carbon fixed (to be discussed below).

The three stations comprising the short meridional transect at 165°E (Table 1) showed that new production was elevated at 2°N relative to the equator and 2°S, as previously observed at 150°W and 140°W (Peña et al., 1992; Wilkerson and Dugdale, 1992; McCarthy et al., 1996). Nitrate uptake rates at 2°N were 2–3 times higher than those at the equator and 2°S and were roughly equivalent to rates measured at the three equatorial stations between the dateline and 170°W. This increased uptake occurred where both nitrate and ammonium concentrations were relatively low, yet chlorophyll concentrations were maximal at the equator (Table 1). Integrated *f*-ratios were depressed at the equator relative to north or south. At 2°N *f*-ratios increased from 0.08 at the surface to a uniform 0.13–0.19 to 80 m and finally to 5.2 at the 0.1% E_0 depth. The *f*-ratio profile at 2°S was similar in pattern to that at the equator, yet with the lowest *f*-ratio found at 0.1% E_0 depths during the cruise with a value of 0.34.

3.3. Flupac Time Series II at 150°W

Chemical and biological conditions sampled in the euphotic zone at 150°W during Flupac from October 19–26, 1994 were not unlike those just east of the dateline during Zonal Flux (Fig. 4). Despite occurring during a moderately warm El Niño event, a sharp salinity front at 172°W separated the highly stratified, oligotrophic warm pool to the west from the weakly stratified, nutrient-rich cold-tongue to the east (Eldin et al., 1997). Nitrate concentrations observed during Time Series II at 150°W were quite uniform, with the 7 μM isopleth remaining at ~115 m and the upper 50 m homogeneous near 3 μM (Fig. 4a). In general both nitrate and temperature exhibited

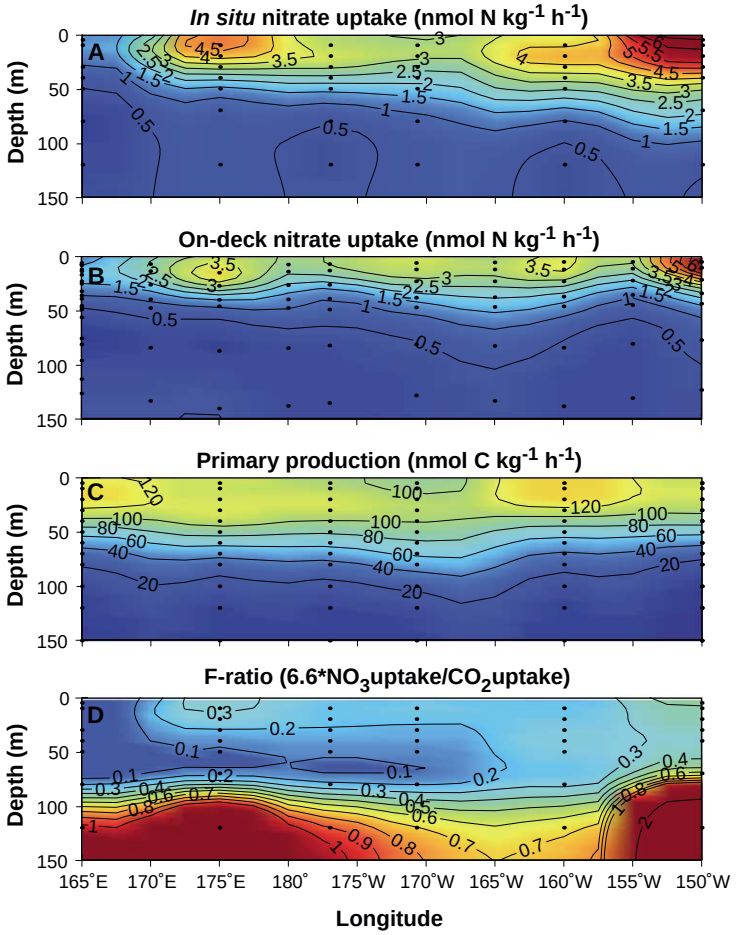

Fig. 3. Zonal Flux contours of (a) nitrate uptake rates, ρNO_3 (nmol N kg^{-1} h^{-1}), measured during in situ incubations, (b) ρNO_3 measured during on-deck incubations, (c) primary production rates courtesy of A. Le Bouteiller (nmol C kg^{-1} h^{-1}), (d) *f*-ratios calculated as $6.6 \times \rho NO_{3-IS}/PP$ at each depth.

much less temporal variability than observed in either EqPac Time Series I or II (Wheeler, 1994; Barber et al., 1996). A nitrite maximum was observed just above the nitracline, similar to Zonal Flux yet with overall higher inventories and appreciable concentrations ($>0.4\,\mu M$) in the upper 50 m for the first 4 days (Fig. 4b). Ammonium was much more vertically homogeneous during Flupac than Zonal Flux, yet showed maximal values and temporal variability similar in magnitude to that observed during EqPac Survey I, EqPac Time Series I and II, and Olipac (Fig. 4c, Table 1) (Aufdenkampe et al., 2001). However, absolute values of ammonium during Flupac may be more uncertain due to difficulties with the method during the cruise.

Chlorophyll concentrations during Flupac never reached the maximum values found during Zonal Flux, but had uniformly high values over the entire upper 70 m that varied little over time (Table 1, Fig. 4c). Primary production also showed little temporal variability when compared with previous time series (Barber et al., 1996), and the higher near-surface chlorophyll translated to greater

depth-integrated primary production rates than observed at any station during Zonal Flux (Table 1, Fig. 5b).

Nitrate uptake rates during the 7-day Flupac time series at 150°W showed substantial variability (Table 1), despite the constancy of nitrate, chlorophyll, and primary production. Contour plots reveal that much of this variability occurred in the upper 40 m (Fig. 5a). Limited sampling below 70 m makes deeper contours nearly meaningless. Daily maximum values of ρNO_3 ranged from 3.4 to 6.7 nM h^{-1}, and depth-integrated new production to 1.0% E_0 ranged from 1.87 to 3.57 mmol N $m^{-2} d^{-1}$ (Table 1). f-Ratios showed considerably more vertical homogeneity than during Zonal Flux, with values near 0.2 everywhere except for the one incubation bottle at 120 m that had a f-ratio of 0.96 (Fig. 5c).

3.4. Diel periodicity of nitrate uptake

Nitrate uptake rates at night, at the four stations during Zonal Flux where they were measured, were consistently an order of magnitude lower at all depths than rates measured in the morning. Thus, at each station the shape of the night-time ρNO_3 profile matched closely that of the day-time profile. When integrated to 1.0% E_0, night-time rates averaged 9% ± 1% of in situ and 12% ± 2% of on-deck day-time integrated rates. A regression of these integrated night-time rates as a function of day-time rates yielded equations $\int \rho_{night} = 0.060 \pm 0.012 \int \rho_{day\ IS} + 5.3 \pm 2.5\ \mu M \quad N\ m^{-2} h^{-1}$ ($r^2 = 0.92$, $p = 0.04$) and $\int \rho_{night} = 0.078 \pm 0.021 \int \rho_{day\ OD} + 5.4 \pm 3.2\ \mu M \quad N\ m^{-2} h^{-1}$ ($r^2 = 0.87$, $p = 0.07$) for in situ and on-deck, respectively. For the eight stations where night rates were not directly measured, there are thus three methods of estimating integrated night-time ρNO_3. One can use the average value for the cruise, use an average ratio, or use a regression. The mean value, 16.8 ± 4.0 μmol $m^{-2} h^{-1}$, exhibits a CV of 24%, the average in situ ratio a CV of 17% and the in situ regression a CV of 8%. Therefore, although previous studies have extrapolated night-time uptake rates by using ratios (McCarthy et al., 1996), the in situ regression was used in this study. However, with such a small sample set, prediction errors were 10–15% (Sokal and Rohlf, 1995).

Although these findings are far from conclusive, they fit well with previous findings. McCarthy et al. (1996) observed a much larger range in the night-to-day uptake ratios, from 6% near the equator to 134% in oligotrophic waters. These ratios seemed to decrease as a function of increasing nitrate inventory and primary production rates, similar to our observation. In the HNLC waters at station P off the coast of British Columbia, Cochlan et al. (1991) recorded ratios of 15–16%, and Probyn et al. (1996) found an inverse relationship between night–day ratios and nitrate across a frontal system off the west coast of southern Africa. This cumulative evidence suggests that day–night contrast may be enhanced in nutrient-rich waters.

Differences between morning and afternoon uptake rates appeared to be minimal during Flupac TS II. The ratios of morning (6 am to noon) uptake rates to full-day (6 am–6 pm) rates averaged 1.1 ± 0.3. Ratios showed neither distinguishable patterns by depth over all days nor between days. Thus, whereas morning rates appeared on average to be 20% higher than afternoon rates, variability was the dominant feature.

3.5. Uncertainty analysis

Understanding the magnitude and sources of uncertainties, especially in a complex measurement, is an important but difficult aspect of all process studies. Here, we use Monte-Carlo error analysis to best estimate how a number of random measurement errors propagate to a calculated uptake rate. Essentially, all the uncertainties in the primary measurements were estimated from observed variability during Zonal Flux and are larger than accepted ideal measurement uncertainties for each method. They therefore explicitly take into account the unavoidable measurement problems encountered in the real world. However, the calculated uncertainties discussed here do not address systematic errors that might bias mean values. Nevertheless, understanding the random errors of a measurement can give substantial

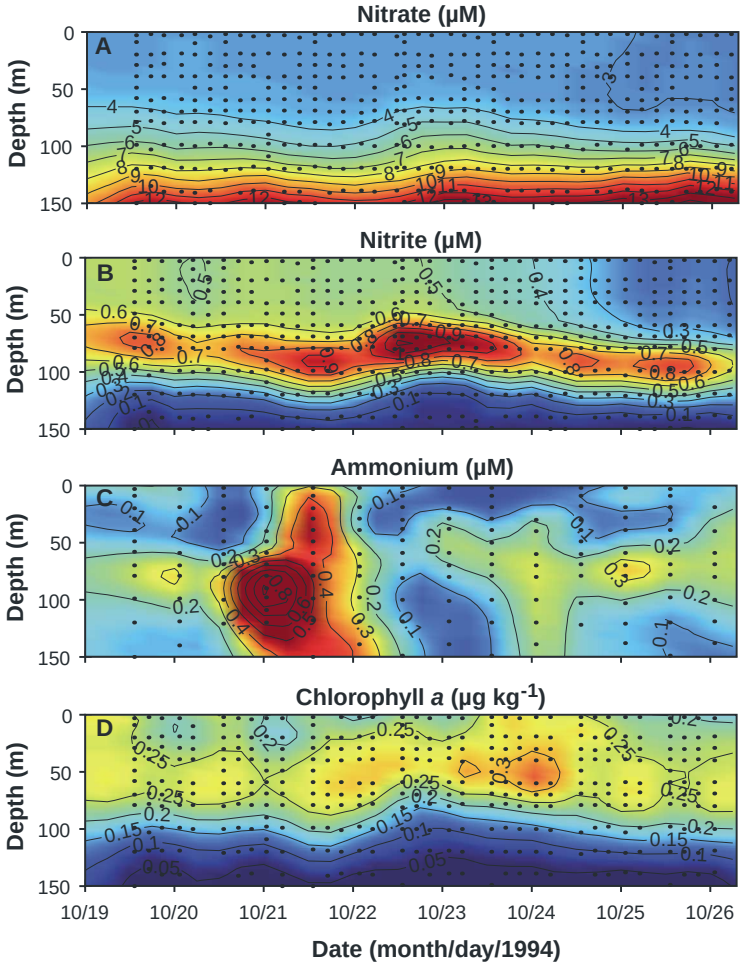

Fig. 4. Flupac contours of (a) nitrate (μM), (b) nitrite (μM), (c) ammonium (μM), and (d) chlorophyll *a* (μg kg^{-1}) concentrations. Due to difficulties with ammonium analyses during Flupac, these ammonium data should be taken with caution.

insight into where the measurement cannot be trusted and also how to improve it.

Uncertainties in nitrate uptake rates (ρNO_3), as estimated by Monte-Carlo error analysis, generally ranged from $\pm 6\%$ to $\pm 20\%$ of the calculated values. These uncertainties increased strongly as calculated ρNO_3 decreased, following a hyperbolic function such that the median uncertainty for the 180 incubations was $\pm 7.6\%$. Rates $> 1.0\,nM\,h^{-1}$ exhibited $< \pm 10\%$ uncertainty. At the very smallest nitrate uptake rates measured ($< 0.15\,nM\,h^{-1}$) at night or at the 0.1% E_0 light level, uncertainties climbed as high as $\pm 100\%$ of the ρNO_3 value.

Uncertainty estimates for depth-integrated uptake rates were much more uniformly distributed. Integrated to the 1% E_0 light level, day-time in situ uptake rate uncertainty averaged $\pm 4.0\%$, with a range of $\pm 3.0\%$ to $\pm 7.1\%$, and on-deck uncertainty averaged $\pm 7.0\%$, with a range of $\pm 5.3\%$ to $\pm 11.6\%$. Absolute uncertainties, in units of μmol $N\,m^{-2}\,h^{-1}$, increased very little with increasing depth of integration. Thus, depth-integrated nitrate uptake rates exhibited smaller relative uncertainties than the ρNO_3 values from which they were calculated. Relative uncertainties for depth-integrated night-time uptake were greater, ranging from 13% to 21%, as a result of the

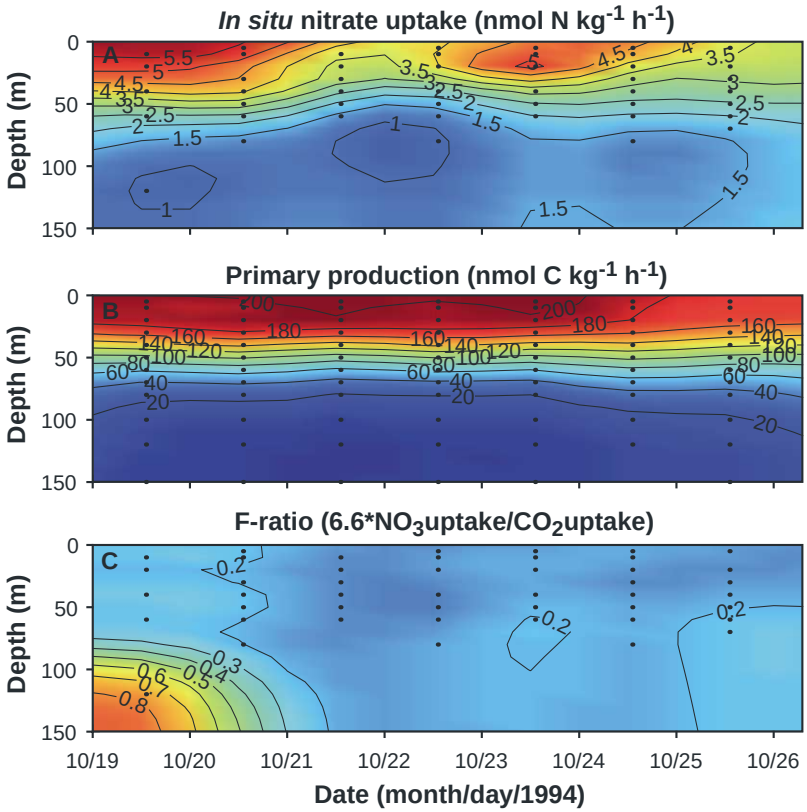

Fig. 5. Flupac contours of (a) nitrate uptake rates, ρNO_3 (nmol N kg^{-1} h^{-1}), measured during in situ incubations, (b) primary production rates courtesy of A. Le Bouteiller (nmol C kg^{-1} h^{-1}), (c) *f*-ratios calculated as $6.6 \times \rho NO_{3-IS}/PP$ at each depth in which both were measured.

much lower absolute uptake rates. Calculation of uncertainties for the regression-estimated night-time rates was not straightforward because the standard prediction error of the regression was much less than errors calculated for measured values. Therefore, a Monte-Carlo simulation was constructed, in which each of the four points were replaced with bivariate normal distributions ($n = 1000$) that matched the mean and standard error for that point. These points were then regressed to obtain a more reasonable standard prediction error. Thus, uncertainties for night rates estimated from regression ranged from $\pm 16\%$ to $\pm 32\%$.

Daily new production uncertainties (day plus night uptake) were little effected by night-time uncertainties because day-time uptake was an order of magnitude larger. Uncertainties in depth-integrated daily new production therefore ranged from $\pm 2.9\%$ to $\pm 7.6\%$ (mean of $\pm 4.3\%$) for in situ incubations, and uncertainties for on-deck incubations ranged from $\pm 5.0\%$ to $\pm 12.7\%$ (mean of $\pm 7.0\%$). Considering a CV of $\pm 20\%$ for in-situ-to-on-deck ratios, daily new production estimated from on-deck incubations (four stations) had uncertainties of $\pm 21\%$ to $\pm 24\%$.

Error sensitivity analysis showed that a doubling of the relatively small uncertainties in measured ^{15}N enrichments ($\pm 1.4\%$) and PON concentrations ($\pm 4.5\%$) within incubations generally had the greatest effect on nitrate uptake and new production uncertainties (Fig. 6). The sensitivity of final uncertainties to these two measurements is quite different at different uptake rates.

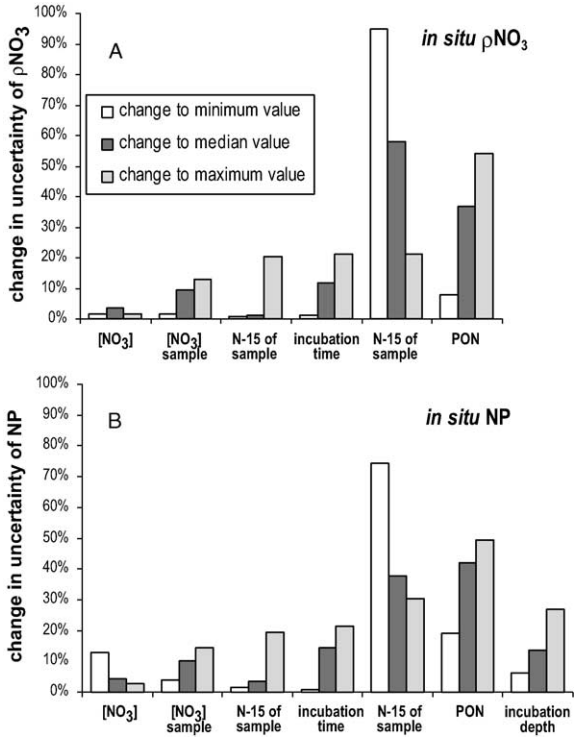

Fig. 6. The increase in calculated total uncertainty by doubling the uncertainty in each individual measurement one at a time, for (a) in situ ρNO_3 and (b) in situ depth-integrated new production. The calculation is performed separately for minimum, median, and maximum values for ρNO_3 and NP, respectively. These values are 0.21, 1.52, and 7.03 nM h^{-1} for ρNO_3 and 0.77, 2.11, and 3.74 mmol N m^{-2} d^{-1} for NP.

At maximum ρNO_3 values, final uncertainties are most sensitive to PON, whereas at minimum ρNO_3, uncertainties in sample ^{15}N enrichments are more important. This Monte-Carlo-based analysis shows that random uncertainties in incubation depths contribute only moderately to overall new production uncertainty. However, systematic uncertainties in incubation depths have a much greater effect. For instance, using the optical model of Morel (1988) for our on-deck incubations would have resulted in underestimates of new production by ~18% because modeled depths were underestimated on average by 18%. Systematic uncertainties in light penetration of on-deck incubators would complicate these uncertainties further (as evidenced by the 30% difference in our on-deck vs. in situ measurements). Therefore, these results still strongly support the conclusions of Barber and Chavez (1991) for primary production—that estimates of depths of light attenuation are likely to be a very significant source of error in any on-deck or "simulated in situ" uptake incubation and could very easily cause 20–30 + % uncertainty in studies with all but the highest quality bio-optical profile measurements.

4. Discussion

4.1. Patterns in nitrate uptake during Zonal Flux and Flupac

Patterns in new production and nitrate uptake rates found during Zonal Flux and Flupac Time Series II were similar to what might be expected in the idealized equatorial Pacific (Barber and Kogelshatz, 1990). The hypothesized zonal gradient of increasing NP to the east was observed and profiles exhibited patterns typical of previous results. However, the range of values observed for both the transect and the time series was surprisingly large. Furthermore, relationships between NP and other biological and chemical water properties were quite different from one cruise to the other.

During the Zonal Flux cruise, new production variability was most strongly correlated to average temperature ($r = -0.79$) and nitrate inventories ($r = 0.73$) in the euphotic zone (Table 2). The fact that these two properties varied almost identically ($r = -0.98$) suggests that physical controls, such as upwelling rates, were rather uniform over the entire transect. Silicate inventory also followed patterns in nitrate inventory as would be expected ($r = -0.79$); however, noticeable differences in the $Si(OH)_4/NO_3$ ratio were present at the stations near the dateline. Ammonium inventories were not uniformly related to NP (or *f*-ratio), but maximums coincided with minimums and vice versa. Chlorophyll inventories were inversely related to nitrate concentrations ($r = -0.64$, $p = 0.03$, $p_{spear} = 0.08$) and marginally to uptake rates ($r = -0.52$, $p = 0.09$, $p_{spear} = 0.30$) (Table 2), but completely unrelated to variability in primary

Table 2
Correlation coefficients, r, of water properties during the Zonal Flux cruise $n = 12$

	New Prod.	Prim. Prod.	Ammonium	Nitrate	Chl	Temp.
New production, 1% E_0	1.00					
Primary production, 0.1% E_0	0.25	1.00				
Ammonium inventory, 1% E_0	−0.40	−0.05	1.00			
Nitrate inventory, 1% E_0	0.73*	0.08	0.12	1.00		
Chlorophyll inventory, 1% E_0	−0.50	0.07	−0.21	−0.64*	1.00	
Temperature average, 1% E_0	−0.79**	−0.10	−0.03	−0.98**	0.65*	1.00

*$p<0.05$, **$p<0.005$.

Table 3
Correlation coefficients, r, of water properties during the Flupac Time Series II $n = 7$

	New Prod.	Prim. Prod.	Ammonium	Nitrate	Chl	Temp.
New production, 1% E_0	1.00					
Primary production, 0.1% E_0	0.42	1.00				
Ammonium inventory, 1% E_0	−0.64	−0.38	1.00			
Nitrate inventory, 1% E_0	0.08	0.31	0.06	1.00		
Chlorophyll inventory, 1% E_0	0.37	0.54	0.08	0.79	1.00	
Temperature average, 1% E_0	0.09	0.06	0.29	−0.44	−0.26	1.00

*$p<0.05$, **$p<0.005$.

production. Lastly, NP and PP were not correlated.

New production variability during Flupac was most strongly related to ammonium inventory of all variables, although not significantly ($r = -0.64$, $p = 0.12$, $p_{spear} = 0.30$) (Table 3), with the lowest integrated rate corresponding to the highest inventory (Table 1). NP was not correlated to PP ($r = 0.42$, $p = 0.35$, $p_{spear} = 0.38$) and was completely unrelated to nitrate inventory or average temperature, which were uncorrelated to each other (Table 3). Chlorophyll inventories were positively correlated to nitrate ($r = 0.79$, $p_{spear} = 0.006$). Although small sample size limits clear interpretation, these results appear to completely contrast findings for Zonal Flux, suggesting that the physical and biogeochemical controls on NP between the two cruises may have been quite different. These contrasting patterns will be discussed in more detail below and in a companion paper (Aufdenkampe and Murray, 2002). As we shall show, when examined in the context of other cruises to the region, Zonal Flux and Flupac appear to have sampled end-members of the processes that control NP in the tropical Pacific.

4.2. Elevated nitrate uptake and f-ratios at depth

One of the most surprising, yet consistent results from these two cruises was the relatively high nitrate uptake rates and enormous f-ratios at the very bottom of the euphotic zone (e.g. 0.1% E_0). It should be noted that because of higher uncertainties nitrate uptake rates at these depths (median CV = 13%, with a range of 6–73%) and carbon uptake (Laws et al., 2000b), f-ratios from 0.1% E_0 are likely to exhibit relatively high uncertainties. Despite this caveat, a number of previously published studies show plots and data suggesting that relatively high nitrate uptake at 0.1% E_0 and below is not uncommon, with minimum values of ρNO_3 often at shallower depths near 1% E_0 (Glibert et al., 1982; Harrison et al., 1983; Murray et al., 1989; Peña et al., 1992; Probyn et al., 1996; Kirchman and Wheeler, 1998). However, few studies have presented their data in such a way that highlights depth specific f-ratios as high as those given here. Indeed, f-ratios calculated according to the second term in Eq. (1) ($\rho NO_3/(\rho NO_3 + \rho NH_4)$), as is often done, cannot exceed one. On the other hand, when f-ratios are

calculated according to the last term of Eq. (1) ($C/N_{redfield} \times \rho NO_3$/carbon uptake), as is done here, there is no mathematical constant on f. In fact, for all four EqPac cruises f-ratios >1 and as high as 43 were in fact quite common at depths >100 m (Aufdenkampe et al., manuscript in preparation; and US JGOFS Web Page, http://www1.whoi.edu/jgofs.html).

A number of issues would need to be considered to explain these observations—locally non-Redfield uptake ratios, other forms of nitrogen uptake (e.g. nitrite, urea, amino acids), non-production related N-uptake by bacteria (Kirchman, 1994), nitrate uptake by vertically migrating plankton (Villareal and Lipschultz, 1995), artifacts of ^{14}C uptake incubations at near zero net production (Laws et al., 2000b), the role of nitrification (Dore and Karl, 1996), etc.—too much to be discussed here adequately. Resolving these issues, and deciding whether or not nitrate uptake at these depths should be included in areal NP estimates, might have a substantial impact on our understanding of upper-ocean nitrogen cycling. The difference in NP obtained from integration to the 0.1% E_0 light levels vs. 1.0% E_0 depths is not negligible (Table 1), and the ratio of the two is nearly constant over the entire sample set at 1.16 ± 0.04. In other words, 12–20% of nitrate uptake in the euphotic zone occurs in the 1.0%–0.1% E_0 depth interval, yet only 4–10% of the primary production occurs in the same interval. Despite this, relatively little attention has been paid to these issues. To address questions of deep and sub-photic nitrate uptake in detail is outside the bounds of this paper, yet these questions deserve serious attention.

4.3. Analysis and estimation of nitrate uptake with MLR

Interpretations of bivariate relationships between new production and other water properties, such as those commonly plotted in previous papers and shown in Tables 2 and 3, can often be severely complicated by issues of cross-correlation between variables (i.e. nitrate and Chl, nitrate and temperature, etc.). These issues are common in uncontrolled systems where many parameters vary simultaneously. One way to aid interpretation is to employ multivariate statistical methods. Of all these techniques, MLR is the simplest and most analogous to the bivariate techniques in common use, and thus provides the most readily interpretable results (Neter et al., 1996). MLR systematically determines which subset of independent variables combine to best explain variability in the chosen variable while taking into account covariance within the independent set. Likewise, partial regression coefficients or slopes, β, and partial correlation coefficients, such as $r_{Y3.12}$, take into account issues of covariance between the independent variables and as a result often reveal very different relations than the commonly calculated simple correlation coefficients that may contain substantial artifacts from cross-correlation. Thus, MLR is particularly suited to the task of examining relationships between many properties that vary simultaneously.

In a synthesis of field data from nine cruises and 121 stations in the tropical Pacific, Aufdenkampe et al. (2001) showed that MLR of areal NP as a function of areal primary production, ammonium inventories, nitrate inventories, and average temperature was able to explain nearly 80% of the variability in NP, better than any other variables from the more than 30 tested (Fig. 7, first line of Table 4). In addition, chlorophyll inventories provided an adequate substitute for primary production in the MLR (first line of Table 5), especially when daily incident surface irradiance was added as an independent variable (Aufdenkampe et al., 2001).

Further analysis here shows that MLR methods are also effective at estimating volumetric nitrate uptake rates (ρNO_3) over all depths to 0.3% E_0 for the six of these same cruises for which depth specific data were available. Subset variable selection again found that primary production, ammonium, nitrate, chlorophyll and temperature were most significantly related to rates of nitrate uptake, together accounting for about 74% of the variability in NP (Fig. 8a). For variables that exhibited values spanning several orders of magnitude, logarithmic transformations were required to fulfill MLR assumptions of normality. The MLR found to best predict nitrate uptake rates

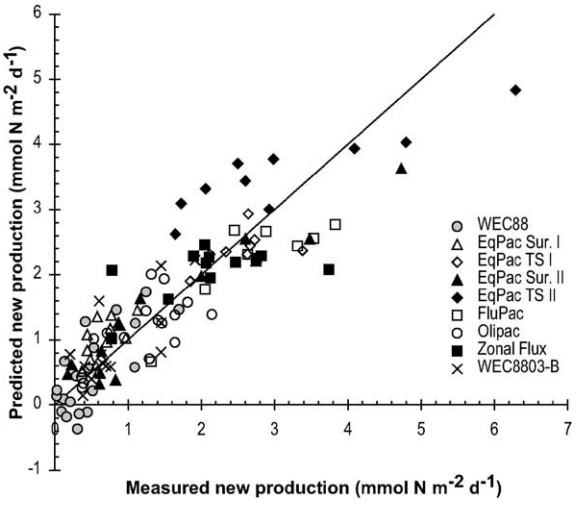

Fig. 7. Depth-integrated new production in the tropical Pacific estimated from multiple linear regressions (MLR) of primary production (PP), ammonia and nitrate, on a per ocean-area basis, for 113 stations sampled during nine cruises ($R^2 = 0.79$, Table 4). MLR fits presented here do not include temperature as an independent variable as in previous studies (Aufdenkampe and Murray, 2002), for better comparison with MLR fits of individual cruises presented in Tables 4 and 5. The line represents a perfect 1:1 fit.

was

$$\log_{10}(\rho NO_3) = -(3.8\pm0.4) + (1.26\pm0.05)\log_{10}[PP] - (0.19\pm0.02)\log_{10}[NH_4] + (0.07\pm0.01)[NO_3] - (0.6\pm0.1)\log_{10}[Chl_a] + (0.03\pm0.01)[\text{temp.}], \quad R^2 = 0.765, \quad n = 357, \tag{3}$$

where units were nmol N kg^{-1} h^{-1} for ρNO_3, nmol C kg^{-1} h^{-1} for PP, μM for ammonium and nitrate, μg kg^{-1} for chlorophyll and °C for temperature. Partial correlation coefficients were 0.82, −0.40, 0.38, −0.25, and 0.12, respectively, with p-values of $<10^{-87}$, 10^{-14}, 10^{-12}, 10^{-5}, and 0.03 for the respective slopes and $p<10^{-22}$ for the intercept. Dropping chlorophyll and temperature from the analysis reduced the fit relatively little (Table 6). However, chlorophyll concentrations, when combined with percent surface irradiance ($\%E_0$), proved to be an adequate substitute for carbon uptake rates, similar to previous findings with depth-integrated data (Fig. 8b, Table 7). In both cases, silicate concentrations proved to be an insignificant variable. Differences in uptake processes at the lowest light levels were elucidated by these MLR analyses. Results presented in Eq. (2) and Tables 6 and 7 all excluded depths below 0.3% E_0. Inclusion of deeper incubations consistently degraded MLR fits ($R^{2*} = 0.64$, $n = 404$ vs. $R^{2*} = 0.76$ for the MLR given in Eq. (2)) with deep points clearly emerging as outliers. Lastly, after appropriate transformations of variables, all MLRs presented here met requirements for effective linearity, homogeneous residuals and normal distributions (see Aufdenkampe et al., 2001, for more detailed discussion). However, because variables were transformed, the bottle-by-bottle MLRs presented here yielded non-linear (i.e. exponential) relationships between original variables.

That nitrate uptake rates at individual depths could be fit by a MLR of a combination of water properties is not intuitive. Each independent variable exhibits its own depth distribution that does not necessarily parallel that of ρNO_3. In the case of nitrate concentrations, the depth trend is opposite, yet all significant partial slopes of nitrate in the MLR are positive (Tables 6 and 7). This is because the inclusion of PP or $\%E_0$ had already accounted for the decreasing trend with depth. Thus, plots of measured vs. predicted profiles of ρNO_3 consistently show good agreement (Fig. 9). Although prediction of individual points were on average ±50% of those measured, values of ρNO_3 span nearly two orders of magnitude (which is not adequately represented in Fig. 8, where ρNO_3 is transformed back into a linear scale). Another observation is that ammonium concentrations show remarkably uniform negative relationships to ρNO_3, consistent with both MLR results of depth-integrated data and with numerous process studies (Dortch, 1990; Wheeler and Kokkinakis, 1990, and many others). Multivariate statistics thus reveals relationships that are often hidden by a bivariate view of the world.

Just as for depth-integrated areal new production, MLR appears to be a robust method of estimating volumetric nitrate uptake rates in the tropical Pacific. These MLR results thus provide an alternate, simple yet robust tool to spatially and temporally extrapolate NP and ρNO_3 from other

Table 4
MLR results from individual cruises, with areal new production (in mmol $N\,m^{-2}\,d^{-1}$) as a function of depth-integrated primary production, ammonium and nitrate inventories

Cruise	n	R^2	R^{2*}	SE	p-value	Intercept		Prim. Prod. (mmol $C\,m^{-2}\,d^{-1}$)			Ammonium (mol m^{-2})			Nitrate (mol m^{-2})		
						$\beta_0 \pm$ SE	p-value	$\beta_1 \pm$ SE	$r_{Y1.23}$	p-value	$\beta_2 \pm$ SE	$r_{Y2.13}$	p-value	$\beta_3 \pm$ SE	$r_{Y3.12}$	p-value
All cruises	100	0.788	0.781	0.576	3×10^{-32}	-0.22 ± 0.14	0.12	0.027 ± 0.002	0.74	2×10^{-18}	-25 ± 7	0.34	0.0005	0.9 ± 0.5	0.18	0.07
WEC88	21	0.601	0.531	0.307	0.001	0.26 ± 0.19	0.20	$7 \times 10^{-04} \pm 5 \times 10^{-04}$	0.32	0.18	-25 ± 14	-0.39	0.10	1.2 ± 0.6	0.46	0.05
WEC8803-B	13	0.793	0.752	0.262	0.0004	-0.15 ± 0.19	0.44	0.011 ± 0.003	0.72	0.008	[a]—	—	—	1.5 ± 0.3	0.84	0.0006
EqPac Sur. I	12	0.473	0.275	0.195	0.14	0.15 ± 0.22	0.51	0.011 ± 0.005	0.60	0.07	-18 ± 8	-0.63	0.05	1.0 ± 1.0	0.34	0.33
EqPac TS I	8	0.593	0.288	0.386	0.26	-1.37 ± 1.79	0.49	0.021 ± 0.014	0.60	0.20	51 ± 40	0.54	0.27	5.5 ± 3.8	0.59	0.22
EqPac Sur. II	14	0.915	0.889	0.455	1×10^{-05}	-0.29 ± 0.32	0.38	0.034 ± 0.008	0.79	0.002	-52 ± 17	-0.70	0.01	1.2 ± 1.3	0.27	0.39
EqPac TS II	10	0.818	0.727	0.774	0.01	-5.94 ± 2.79	0.08	0.005 ± 0.002	0.75	0.03	-25 ± 70	-0.14	0.73	2.7 ± 4.3	0.25	0.55
OliPac	15	0.683	0.597	0.337	0.004	0.53 ± 0.34	0.15	0.004 ± 0.008	0.14	0.65	-4 ± 15	-0.08	0.81	4.4 ± 1.6	0.63	0.02
Flupac TS II	7	0.451	-0.097	0.664	0.56	-0.55 ± 8.72	0.95	0.033 ± 0.088	0.21	0.73	-32 ± 26	-0.58	0.31	1.9 ± 15.6	0.07	0.91
Zonal Flux	12	0.805	0.732	0.431	0.003	-0.47 ± 1.05	0.67	0.012 ± 0.011	0.35	0.32	-52 ± 17	-0.73	0.02	7.8 ± 1.6	0.87	0.001

Note: R^{2*} represents the adjusted R^2. SE represents the standard error of new production estimates and of regression coefficients (slopes), β. Partial correlation coefficients of NP with each independent variable are denoted by $r_{Y1.23}$, etc.

[a] Ammonium was not included in the MLR for WEC8803-B, because no data were available.

Table 5
MLR results from individual cruises, with areal new production as a function of chlorophyll, ammonium and nitrate inventories

Cruise	n	R^2	R^{2*}	SE	p-value	Intercept		Chlorophyll (mg m^{-2})			Ammonium (mol m^{-2})			Nitrate (mol m^{-2})		
						$\beta_0 \pm$ SE	p-value	$\beta_1 \pm$ SE	$r_{Y1.23}$	p-value	$\beta_2 \pm$ SE	$r_{Y2.13}$	p-value	$\beta_3 \pm$ SE	$r_{Y3.12}$	p-value
All cruises	104	0.612	0.601	0.764	2×10^{-20}	−0.73±0.33	0.03	0.106±0.022	0.44	4×10^{-06}	−23±9	0.24	0.01	2.0±0.7	0.29	0.003
WEC88	21	0.594	0.523	0.310	0.001	−0.22±0.52	0.68	0.025±0.019	0.30	0.21	−21±16	−0.31	0.20	1.4±0.5	0.52	0.02
WEC8803-B	13	0.610	0.533	0.360	0.009	−0.45±0.78	0.58	0.037±0.036	0.31	0.33	[a]—	—	—	1.4±0.4	0.72	0.009
EqPac Sur. I	12	0.220	−0.073	0.237	0.55	0.23±0.49	0.65	0.015±0.022	0.24	0.51	−13±10	−0.43	0.21	1.6±1.2	0.44	0.21
EqPac TS I	8	0.360	−0.119	0.485	0.58	0.27±2.78	0.93	0.007±0.088	0.04	0.94	71±56	0.54	0.27	5.5±4.9	0.48	0.33
EqPac Sur. II	14	0.817	0.762	0.667	0.001	−0.29±0.64	0.66	0.063±0.040	0.45	0.14	−42±26	−0.45	0.14	3.7±1.7	0.57	0.05
EqPac TS II	10	0.689	0.533	1.012	0.06	−5.63±4.08	0.22	0.079±0.056	0.50	0.21	−49±92	−0.21	0.61	10.9±4.7	0.69	0.06
OliPac	19	0.631	0.557	0.324	0.002	1.15±0.50	0.03	−0.029±0.040	−0.18	0.49	−4±14	−0.07	0.80	5.4±1.6	0.65	0.005
Flupac TS II	7	0.712	0.424	0.481	0.238	−0.44±3.32	0.90	0.420±0.243	0.71	0.18	−37±17	−0.78	0.12	−19.7±17	−0.55	0.34
Zonal Flux	12	0.797	0.721	0.439	0.004	2.26±2.01	0.29	−0.071±0.080	−0.30	0.40	−55±18	−0.74	0.01	6.8±2.1	0.76	0.01

[a] Ammonium was not included in the MLR for WEC8803-B, because no data were available.

measured water properties. Unlike other regions of the world, *f*-ratios in the tropical Pacific do not appear to be a simple function of any simple water property (Eppley and Peterson, 1979; Platt and Harrison, 1985; Harrison et al., 1987; Laws et al., 2000a). The lack of consistent *f*-ratio relationships is apparent on a volumetric, bottle-by-bottle basis (Fig. 10), just as from areal, depth-integrated data (Fig. 2 in Aufdenkampe et al., 2001). Therefore, within the tropical Pacific region, it is clear that multiplying modeled or measured estimates of primary productivity by estimated *f*-ratios would lead to considerable errors in NP or ρNO_3 estimates. Simple *f*-ratio approaches simply cannot capture the substantial variability in nitrate uptake rates observed within the tropical Pacific (Fig. 10). On the other hand, MLR cross-validation analysis confirms the robustness of the MLR-based approach to predict NP for other data sets, with prediction uncertainties of only 10–50% for all but the lowest NP fluxes (Aufdenkampe et al., 2001). Thus, the MLR-based estimations of NP from ship-based and potentially remotely sensed data provide a powerful alternative to other popular simple methods.

4.4. MLR as a tool to study controls on new production: variability in nitrate response revealed

MLR, just as any statistical technique, cannot determine cause and effect relationships. It can, however, potentially provide a powerful tool to survey patterns of variability within a natural system. When simple or partial correlations are elucidated between properties of that system, these effective relationships in fact may just be acting as proxies for the real controls on the process of interest. These underlying controls—such as iron fluxes, ecosystem dynamics, etc.—may be much more difficult to quantify. Yet, if the relationships between an underlying control and its proxies are understood, the proxies can themselves become an essential link to understanding the functioning of the system. Therefore, patterns of variability are examined here with the goal of linking observations of simple water properties to underlying controls, which is expanded on with a simple

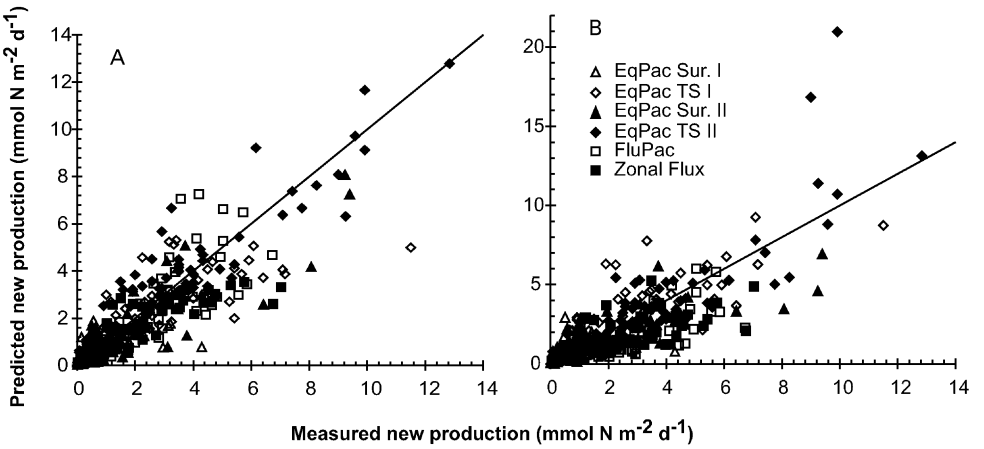

Fig. 8. Depth-specific nitrate uptake rates in the tropical Pacific estimated from MLR of $\log(\rho NO_3)$ as a function of (a) log(PP), log(ammonium), nitrate, log(chl), and temperature, on a per volume basis, for 357 incubations ($R^2 = 0.74$ when transformed back to a linear scale, Table 6), or as a function of (b) $\log(\%E_0)$, log(chl), log(ammonium), nitrate, and temperature, on a per volume basis, for 381 incubations ($R^2 = 0.63$ when transformed back, Table 7). Care was given to insure that that all water property data came from bottles collected as close as possible in time and depth as nitrate uptake collections. Nutrients required linear interpolation to the correct depths for all cruises except Zonal Flux, where all relevant samples were collected with the same casts. Data from depths corresponding to $<0.3\%$ E_0 appear as outliers and were excluded. Lines represent a perfect 1:1 fit.

mechanistic model in the following paper (Aufdenkampe and Murray, 2002).

The fact that single MLR equations can explain new production or nitrate uptake rates over the entire range observed in the region and over such a wide range of oceanographic conditions demonstrates a certain uniformity in relationships of each water property with NP. However, inspection of the fit suggests that individual cruises may have systematic differences in these relationships (Fig. 7). Whereas all MLR models have a tendency to over-predict highest values (the multiple R^2 is always equal to the slope of the regression of predicted as a function of measured values), some cruises do have skewed predictions relative to the general trend. For instance, NP at individual stations during Zonal Flux or EqPac TS II are not predicted very well with the MLR derived from all cruises. Inspection of scatter plots of each property vs. NP and vs. standard residuals (Fig. 4 in Aufdenkampe et al., 2001) suggests that this is due to certain properties, in particular nitrate, having varying relationships to NP from one cruise to the next. Understanding different MLR responses for each cruise has the potential to yield useful clues about how the processes that controlled NP differed between cruises.

To compare differences in the relative importance and partial slope of each euphotic zone property within and between cruises, areal NP values were fit with MLR for each individual cruise (Tables 4 and 5). Regressions were all made against primary production (or chlorophyll), ammonium and nitrate for comparison, although including all three variables did not always produce the best fit due to limited sample size. Changes in the number of variables, choice of variables, or the slope of one variable can change the slopes of the other variables. For these reasons temperature was excluded. Even though it is a significant variable in the MLR of all 121 stations, the inclusion of temperature almost always degraded the MLR fits for individual cruises, making other coefficients more difficult to interpret. For some cruises, integrating one or more of the variables to the 0.1% E_0 depths improved statistical significance of the fit, but all MLRs considered here were performed on nutrient and chlorophyll inventories to 1.0% E_0 depths, and primary production to 0.1% E_0, for consistency.

Table 6
MLR results from individual cruises on a bottle-by-bottle basis, with $\log_{10}(\int NO_3)$ as a function of $\log_{10}$ (primary production), $\log_{10}$ (ammonium) and nitrate

					Intercept		log(PP) (nmol C kg^{-1} h^{-1})			log(Ammonium) (μM)			Nitrate (μM)		
Cruise	n	R^2	R^{2*}	SE	$\beta_0 \pm$ SE	p-value	$\beta_1 \pm$ SE	$r_{Y1.23}$	p-value	$\beta_2 \pm$ SE	$r_{Y2.13}$	p-value	$\beta_3 \pm$ SE	$r_{Y3.12}$	p-value
All cruises	357	0.745	0.743	0.284	-1.50 ± 0.06	8×10^{-89}	1.19 ± 0.04	0.83	8×10^{-93}	-0.22 ± 0.02	-0.45	2×10^{-19}	0.04 ± 0.01	0.33	2×10^{-10}
EqPac Sur. I	71	0.567	0.547	0.336	-2.84 ± 0.28	2×10^{-15}	1.27 ± 0.14	0.73	7×10^{-13}	-0.41 ± 0.10	-0.43	2×10^{-04}	0.03 ± 0.03	0.11	0.38
EqPac TS I	56	0.724	0.708	0.201	-1.43 ± 0.63	3×10^{-02}	0.94 ± 0.26	0.45	6×10^{-04}	-0.11 ± 0.06	-0.26	0.06	-0.06 ± 0.06	-0.13	0.35
EqPac Sur. II	68	0.807	0.798	0.263	-2.56 ± 0.17	6×10^{-23}	0.95 ± 0.09	0.80	4×10^{-16}	-0.40 ± 0.05	-0.74	8×10^{-13}	0.12 ± 0.01	0.76	2×10^{-13}
EqPac TS II	69	0.793	0.783	0.235	-3.23 ± 0.35	2×10^{-13}	1.45 ± 0.11	0.86	2×10^{-20}	-0.11 ± 0.07	-0.19	0.11	0.08 ± 0.03	0.33	0.01
Flupac TS II	45	0.805	0.790	0.122	-0.93 ± 0.39	0.02	0.78 ± 0.10	0.78	1×10^{-10}	-0.07 ± 0.04	-0.29	0.06	-0.10 ± 0.08	-0.20	0.19
Zonal Flux	48	0.861	0.851	0.21	-3.19 ± 0.21	4×10^{-19}	1.36 ± 0.10	0.90	2×10^{-17}	-0.32 ± 0.08	-0.50	4×10^{-04}	0.12 ± 0.02	0.64	2×10^{-06}

Because variables were first log-transformed to better fit a normal distribution, regression coefficients β, correspond to exponents of the corresponding non-transformed variables.

Table 7
MLR results from individual cruises on a bottle-by-bottle basis, with $\log_{10}(\int NO_3)$ as a function of $\log_{10}(\%E_0)$, $\log_{10}$ (chl), $\log_{10}$ (ammonium), nitrate and temperature

Cruise	n	R^2	R^{2*}	SE	Intercept		$\log_{10}(\%E_0)$[a]			$\log_{10}$(Chlorophyll) (μg kg^{-1})			$\log_{10}$ (Ammonium) (μM)			Nitrate (μM)			Temperature (°C)		
					$\beta_0 \pm$ SE	p-value	$\beta_1 \pm$ SE	$r_{Y1.2345}$	p-value	$\beta_2 \pm$ SE	$r_{Y2.1345}$	p-value	$\beta_3 \pm$ SE	$r_{Y3.1245}$	p-value	$\beta_4 \pm$ SE	$r_{Y4.1235}$	p-value	$\beta_5 \pm$ SE	$r_{Y5.1234}$	p-value
All cruises	381	0.679	0.674	0.317	-2.90 ± 0.39	1×10^{-12}	0.63 ± 0.03	0.75	4×10^{-70}	0.88 ± 0.12	0.34	1×10^{-11}	-0.14 ± 0.03	-0.27	7×10^{-08}	0.12 ± 0.01	0.51	7×10^{-26}	0.08 ± 0.01	0.32	2×1^{-10}
EqPac Sur. I	71	0.616	0.587	0.321	-2.67 ± 0.70	3×10^{-4}	0.59 ± 0.08	0.66	1×10^{-09}	1.33 ± 0.32	0.46	8×10^{-05}	-0.45 ± 0.12	-0.42	5×10^{-04}	0.07 ± 0.03	0.28	0.02	0.08 ± 0.02	0.39	0.001
EqPac TS I	56	0.763	0.739	0.19	3.29 ± 2.77	0.24	0.46 ± 0.11	0.50	2×10^{-04}	-0.19 ± 0.28	-0.09	0.51	-0.12 ± 0.07	-0.24	0.08	-0.10 ± 0.07	-0.20	0.15	-0.12 ± 0.10	-0.18	0.21
EqPac Sur. II	68	0.818	0.803	0.259	-5.77 ± 1.35	7×10^{-05}	0.58 ± 0.06	0.79	5×10^{-15}	1.27 ± 0.27	0.52	1×10^{-05}	-0.36 ± 0.06	-0.63	2×10^{-08}	0.21 ± 0.02	0.76	3×10^{-13}	0.18 ± 0.05	0.41	0.001
EqPac TS II	69	0.776	0.758	0.249	-5.99 ± 3.53	9×10^{-02}	0.72 ± 0.08	0.75	6×10^{-13}	0.51 ± 0.27	0.24	0.06	-0.14 ± 0.07	-0.24	0.05	0.15 ± 0.05	0.35	0.005	0.19 ± 0.13	0.18	0.15
Flupac TS II	45	0.835	0.814	0.115	-17.6 ± 5.7	4×10^{-03}	0.26 ± 0.04	0.68	8×10^{-07}	-0.57 ± 0.42	-0.21	0.18	-0.12 ± 0.03	-0.48	0.002	0.07 ± 0.11	0.10	0.52	0.62 ± 0.19	0.46	0.002
Zonal Flux	72	0.797	0.781	0.239	-0.08 ± 1.84	0.96	0.77 ± 0.05	0.86	2×10^{-21}	1.05 ± 0.34	0.35	0.003	-0.21 ± 0.09	-0.28	0.02	0.15 ± 0.04	0.43	2×10^{-04}	-0.02 ± 0.06	-0.04	0.72

[a] $\%E_0$ represents the percent of incident surface radiation that reaches the collection or incubation depth.

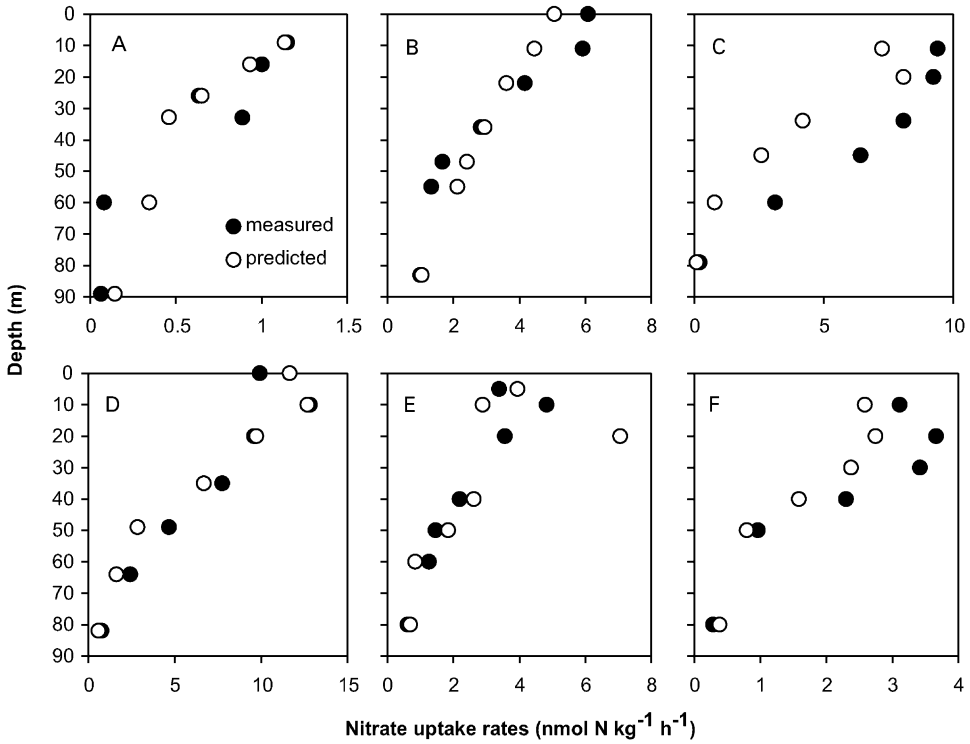

Fig. 9. Profiles of measured nitrate uptake rates with the corresponding rates predicted from the MLR given by Eq. (3) and Fig. 8A. Data come from (a) EqPac Survey I, equator; (b) EqPac TS I, April 2; (c) EqPac Survey II, 2°N; (d) EqPac TS II, October 10; (e) Flupac TS II, October 22; (f) Zonal Flux, 177°W. These six stations to were chosen to be representative of the patterns of error typical of all 63 stations analyzed. Several predicted values lie directly on top of their corresponding measured values, hiding them in these figures.

Therefore, the presentation of MLR results in Tables 4 and 5 was specifically designed to aid comparisons between cruises. These results do not serve the purpose of predicting NP for individual cruises.

In general, the fits (R^2) are as good within individual cruises as for the MLR of all cruises (Tables 4 and 5), although R^{2*} and the significance of regression coefficients are often substantially reduced due to small sample sizes. Partial correlation coefficients are thus especially useful for comparisons of relative importance of independent variables between cruises, where differing small sample sizes make p-values a biased indicator. However, many of the MLR relationships are not statistically significant, and as such we caution against over-interpretation of all variables for any cruise, especially given that we have presented all three variables even when inclusion all three degrades the MLR fit. Despite this, there are general patterns in the results that are apparent. Inspection of partial correlation coefficients in Tables 4 and 5 reveals substantial heterogeneity in the responses of NP to other properties. In the MLR of all cruises, primary production (or chlorophyll) was clearly the dominant variable, yet when cruises were analyzed individually, variability in NP was most strongly associated to variability in nitrate during WEC88, WEC8803-B, Olipac and Zonal Flux, and ammonium was most important during EqPac Survey I and Flupac (although not significantly so for the latter). The shift in importance from chlorophyll to nitrate was even more pronounced, with seven of the nine cruises exhibiting their highest partial correlations of NP to nitrate and none to chlorophyll. It

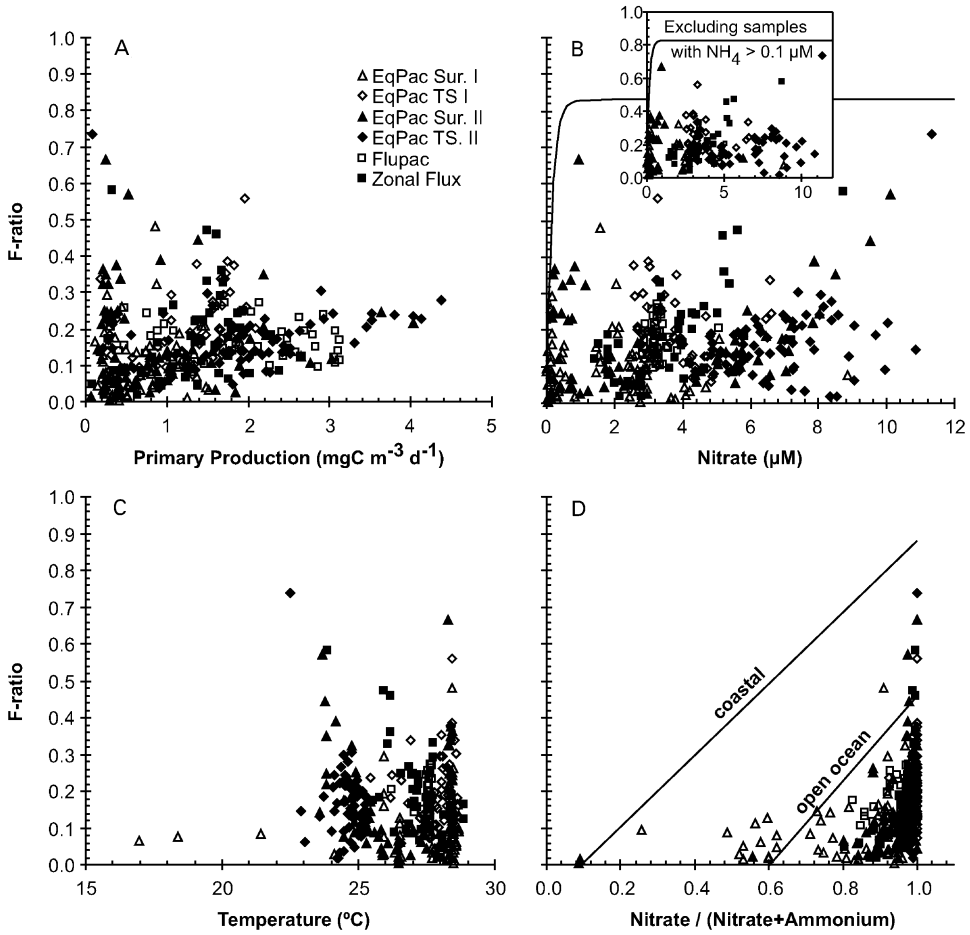

Fig. 10. Scatter plots showing measured f-ratios in the tropical Pacific on a bottle-by-bottle basis ($n = 357$) as a function of (a) measured primary production rates, (b) nitrate concentrations, (c) temperature, and (d) the ratio of nitrate to the sum of nitrate and ammonium. Shown in (b) and (d) are lines representing the relationships found in previous studies for other regions by Platt and Harrison (1985) and Harrison et al. (1987), respectively. The data set presented in these figures is identical to that in Fig. 8a. All f-ratios presented in this paper are calculated as the ratio of measured $^{15}NO_3$ uptake rates to primary production rates multiplied by a molar C/N of 6.6.

appears that primary production (or chlorophyll) was the "least common denominator" when all cruises were lumped together, yet variability in nitrate may be at least as important or more so when cruises are examined individually. In other words, the patterns of within cruise variability are different from the patterns of between cruise variability.

These patterns can be further examined by comparison of partial slopes for each MLR. However, a caveat must first be made. MLR is a method for predicting a Y from many Xs, but when those Xs have measurement and other inherent errors, MLR does not give unbiased estimates of the real "functional" relationships (or slopes) between each of those Xs and Y. This situation is analogous to that of simple linear regression. However, unlike the bivariate case where unbiased relationships can be estimated with various Model II methods, no method exists

for determining unbiased partial slopes for MLR (Ricker, 1973; Rayner, 1985; Sokal and Rohlf, 1995). A Monte-Carlo simulation was thus performed to determine whether potential biases might affect our comparisons of slopes. Random values for PP, ammonium, and nitrate (normally distributed with representative standard deviations) were used to calculate NP values according to the first equation in Table 4. All values were then corrupted with random errors representing the maximum likely error for each variable. MLR on this simulated dataset did produce slopes that were underestimates of values obtained from MLR of the real data. However, the calculated SE of these slopes (from real data, Tables 4 and 5) were proportional to these biases (calculated from Monte Carlo simulation) for a given sample size. Therefore, expected values for each slope always fell within the range predicted by MLR (i.e. $\beta \pm \mathrm{SE}$) for $n < 100$. Furthermore, reducing the range of any X, which is the most likely source of bias to these analyses, increased the SE such that expected values still fell within the ranges predicted by MLR. Thus, for small sample sizes such as those in Tables 4 and 5 ($n < 21$), it is extremely unlikely that differences in slopes between cruises that are smaller than their associated SE could result from these Model I type slope biases. For instance, it is valid to conclude that the partial nitrate slope for Zonal Flux (7.8 ± 1.6) was greater than for Olipac (4.4 ± 1.6), which was greater than for WEC88 (1.2 ± 0.6). On the other hand, little can be concluded about the nitrate slopes of EqPac TS I, TS II or Flupac. Although it is not possible to determine the true slopes for relationships of NP to other properties with MLR, it is possible to determine which slopes are different between cruises.

Keeping this caveat in mind, inspection of slopes along with their associated SE suggested that the response of NP to nitrate differed more between cruises than the response to any other variable (Tables 4 and 5). Only primary production came close. Further MLR analysis revealed, however, that variability in new-to-primary-production slopes were likely due to differences in plankton community composition between cruises. Addition of HPLC pigment derived estimates of diatom-associated chlorophyll, which were only measured during EqPac (Bidigare and Ondrusek, 1996), to the individual MLRs of the EqPac cruises brings the new-to-primary-production slopes consistently to values of 0.010 ± 0.006 mol N uptake per mole C uptake. However, large differences in the new-production-to-nitrate slopes remained for these cruises. Additional evidence for the high variability of the NP response to nitrate was that the mean nitrate slope from individual cruises was much larger than the slope found in the "all cruises" MLR. In contrast, the responses of PP, ammonium, and chlorophyll during individual cruises all center on the "all cruises" values. Lastly, a MLR simulation was run on all 100 stations (Table 4) such that the nitrate values for each individual cruise were treated as different independent variables (with their own slopes) while PP and ammonium remained one variable for all 100 stations. This simulation was repeated for PP and ammonium in turn, and likewise for the chlorophyll MLR of Table 5. In both sets of simulations, the most significant MLRs were that in which nitrate responses were separated by cruise ($R^{2*} = 0.826$ vs. 0.819 vs. 0.819 for nitrate, PP, and ammonium, respectively, and $R^{2*} = 0.802$ vs. 0.777 vs. 0.729 for nitrate, chlorophyll, and ammonium, respectively).

Therefore, multiple lines of evidence all suggest that NP exhibits considerable inter-cruise variability in its response to nitrate, more than any other water property considered in this MLR analysis. What might be the cause for this variable response between cruises? Nitrate has in the past been considered a proxy for iron because they share the same primary source in the tropical Pacific, the Equatorial Undercurrent (Gordon et al., 1997). If so, why is it a better proxy for within cruise variability than between cruise variability? Examination of Zonal Flux and Flupac Time Series II may lead to insights. In all the discussions above, these cruises represent each extreme. NP during Zonal Flux exhibited the strongest response to nitrate of all the cruises (with the possible exception of EqPac TS II), and Flupac TS II the weakest (Tables 4–7). Both cruises sampled similar water masses with weak diatom activity (Dunne et al., 1999), yet with such large

differences in NP response they are the perfect vehicle in which to explore possible controls on these differences. Such an exploration is taken up in the companion paper (Aufdenkampe and Murray, 2002).

5. Conclusions

The ability to remotely monitor ecosystem changes controlling the world's major biogeochemical cycles will be a requirement in future efforts to assess and manage our impact to the global system. Oceanographic new production plays an important role in the global carbon cycle, especially with respect to HNLC environments, where the delayed uptake of upwelled macronutrients results in significant out-gassing of CO_2 to the atmosphere (Murray et al., 1994). The high variability of many processes in the tropical Pacific, such as new production, suggests that this region deserves special attention. The results of this study make several steps toward achieving the goals of understanding and even monitoring new production in this region.

New nitrate uptake rates presented here expand existing data for the region. Zonal Flux provided the first zonal transect of these processes in the tropical Pacific, and Flupac TS II yielded an equatorial time-series during conditions unique to those previously sampled. These measurements highlight the large variability in new production rates and *f*-ratios, and in their relationships with other water properties, that have been observed in the tropical Pacific region during seven previous studies. In addition, the first detailed uncertainty analysis for these methods provide confidence in these and previous measurements, and provides direction for future efforts at limiting uncertainties.

Multiple linear regression analysis of the nine cruises revealed that the large variability in measured new production in the tropical Pacific is far from random. This study strengthens previous results (Aufdenkampe et al., 2001) showing that the individual relationships of nitrate uptake rates to primary production, chlorophyll, ammonium, nitrate, and temperature are all quite uniform over the wide range of hydrographic and ecological conditions found in tropical Pacific region, once variability in the other variables is taken into account. These MLR results therefore offer a robust statistical method for extrapolating both depth-integrated new production and depth-specific nitrate uptake estimates to wider temporal and spatial scales from commonly measured properties. Furthermore, MLR provided a method of examining patterns of variability within a system containing many inter-correlated variables. Such examination clearly elucidated the strong negative response of NP to ammonium and also revealed that the relationship of NP to nitrate exhibited substantial variability between cruises. Zonal Flux and Flupac TS II represented each extreme of this variability, offering examples with which to explore the underlying causes for such different responses (Aufdenkampe and Murray, 2002).

Acknowledgements

We thank the crew and scientists aboard the R./V. *Thomas G. Thomson* and the R./V. *Atalante* for their good cheer, assistance and thoughtful discussion at sea. Statistical Consulting Services at the University of Washington's Department of Statistics provided invaluable help with MLR analyses. Many thanks to A. Le Bouteiller, R.T. Barber, Z. Johnson, and S. Pegau sharing their data, and to W. Gentleman, J.I. Hedges, E. Laws, J. Newton and two anonymous reviewers for encouragement and comments on the manuscript. R. Le Borgne and T. Platt deserve special thanks for their editorial handling of this manuscript. This work was funded by NSF grant OCE 9504202. This is US JGOFS contribution No. 618.

References

Aufdenkampe, A.K., Murray, J.W., 2002. Controls on new production: the role of iron and physical processes. Deep-Sea Research II 49, 2649–2668.

Aufdenkampe, A.K., McCarthy, J.J., Rodier, M., Navarette, C., Dunne, J.P., Murray, J.W., 2001. Estimation of new

production in the tropical Pacific. Global Biogeochemical Cycles 15, 101–113.

Barber, R.T., Chavez, F.P., 1991. Regulations of primary productivity rate in the equatorial Pacific. Limnology and Oceanography 36, 1803–1815.

Barber, R.T., Kogelshatz, J.E., 1990. Nutrients and productivity during the 1982/83 El Niño. In: Glynn, P.W. (Ed.), Global Consequences of the 1982/83 El Niño-Southern Oscillation Event. Elsevier, New York, pp. 21–53.

Barber, R.T., Borden, L., Johnson, Z., 1997. Ground truthing modeled kpar and on deck primary productivity incubations with in situ observations. Ocean Optics XIII, 834–839.

Barber, R.T., Sanderson, M.P., Lindley, S.T., Chai, F., Newton, J., Trees, C.C., Foley, D.G., Chavez, F.P., 1996. Primary productivity and its regulation in the equatorial Pacific during and following the 1991–1992 El Niño. Deep-Sea Research II 43, 933–969.

Bidigare, R.R., Ondrusek, M.E., 1996. Spatial and temporal variability of phytoplankton pigment distributions in the central equatorial Pacific Ocean. Deep-Sea Research II 43, 809–833.

Bonnet, S., 1995. Manuel d'analyses chimiques dans l'eau de mer. Vol. 2, ORSTOM-Nouméa, Notes Techniques Sciences de la Mer, Océanographie.

Chavez, F.P., Buck, K.R., Service, S.K., Newton, J., Barber, R.T., 1996. Phytoplankton variability in the central and eastern tropical Pacific. Deep-Sea Research II 43, 835–870.

Cochlan, W.P., Harrison, P.J., Denman, K.L., 1991. Diel periodicity of nitrogen uptake by marine phytoplankton in nitrate-rich environments. Limnology and Oceanography 36, 1689–1700.

Dore, J.E., Karl, D.M., 1996. Nitrification in the euphotic zone as a source of nitrite, nitrate, and nitrous oxide at Station ALOHA. Limnology and Oceanography 41, 1619–1628.

Dortch, Q., 1990. The interaction between ammonium and nitrate uptake in phytoplankton. Marine Ecology Progress Series 61, 183–201.

Dugdale, R.C., Goering, J.J., 1967. Uptake of new and regenerated forms of nitrogen in primary productivity. Limnology and Oceanography 12, 196–206.

Dugdale, R.C., Wilkerson, F.P., 1986. The use of ^{15}N to measure nitrogen uptake in eutrophic oceans; experimental considerations. Limnology and Oceanography 31, 673–689.

Dugdale, R.C., Wilkerson, F.P., Barber, R.T., Chavez, F.P., 1992. Estimating new production in the equatorial Pacific Ocean at 150°W. Journal of Geophysical Research 97, 681–686.

Dunne, J.P., Murray, J.W., Aufdenkampe, A.K., Blain, S., Rodier, M., 1999. Silicon–nitrogen coupling in the equatorial Pacific upwelling zone. Global Biogeochemical Cycles 13, 715–726.

Dunne, J.P., Murray, J.W., Rodier, M., Hansell, D.A., 2000. Export production in the western and central equatorial Pacific: zonal and temporal variability. Deep-Sea Research I 47, 901–936.

Eldin, G., Rodier, M., Radenac, M.-H., 1997. Physical and nutrient variability in the upper equatorial Pacific associated with westerly wind forcing and wave activity in October 1994. Deep-Sea Research II 44, 1783–1800.

Eppley, R.W., Peterson, B.J., 1979. Particulate organic matter flux and planktonic new production in the deep ocean. Nature 282, 677–680.

Falkowski, P.G., Barber, R.T., Smetacek, V., 1998. Biogeochemical controls and feedbacks on ocean primary production. Science 281, 200–206.

Feely, R.A., Wanninkhof, R., Goyet, C., Archer, D.E., Takahashi, T., 1997. Variability of CO_2 distributions and sea–air fluxes in the central and eastern equatorial Pacific during the 1991–1994 El Niño. Deep-Sea Research II 44, 1851–1867.

Fitzwater, S.E., Coale, K.H., Gordon, R.M., Johnson, K.S., Ondrusek, M.E., 1996. Iron deficiency and phytoplankton growth in the equatorial Pacific. Deep-Sea Research II 43, 995–1015.

Gardner, W.D., Chung, S.P., Richardson, M.J., Walsh, I.D., 1995. The oceanic mixed-layer pump. Deep-Sea Research II 42, 757–775.

Glibert, P.M., Biggs, D.C., McCarthy, J.J., 1982. Utilization of ammonium and nitrate during austral summer in the Scotia Sea. Deep-Sea Research 29, 837–850.

Gordon, R.M., Coale, K.H., Johnson, K.S., 1997. Iron distributions in the equatorial Pacific: implications for new production. Limnology and Oceanography 43, 419–431.

Grasshoff, K., Ehrhardt, M., Kremling, K., 1983. Methods of Seawater Analysis. Verlag Chimie, Kiel, p. 419.

Guiraud, G., Fardeau, J.C., 1980. Détermination isotopique par spectrométrie optique de composés faiblement enrichis en azonte-15. Analysis 8, 148–152.

Harrison, W.G., Douglas, D., Falkowski, P.G., Rowe, G., Vidal, J., 1983. Summer nutrient dynamics of the Middle Atlantic Bight: nitrogen uptake and regeneration. Journal of Plankton Research 5, 539–556.

Harrison, W.G., Platt, T., Lewis, M.R., 1987. F-ratio and its relationship to ambient nitrate concentration in coastal waters. Journal of Plankton Research 9, 235–248.

Kirchman, D.L., 1994. The uptake of inorganic nutrients by heterotrophic bacteria. Microbial Ecology 28, 255–271.

Kirchman, D.L., Wheeler, P.A., 1998. Uptake of ammonium and nitrate by heterotrophic bacteria and phytoplankton in the sub-Arctic Pacific. Deep-Sea Research I 45, 347–365.

Kurz, K.D., Maier-Reimer, E., 1993. Iron fertilization of the Austral Ocean: the Hamburg Model assessment. Global Biogeochemical Cycles 7, 229–244.

Landry, M.R., Barber, R.T., Bidigare, R.R., Chai, F., Coale, K.H., Dam, H.G., Lewis, M.R., Lindley, S.T., McCarthy, J.J., Roman, M.R., Stoecker, D.K., Verity, P.G., White, J.R., 1997. Iron and grazing constraints on primary production in the central equatorial Pacific: an EQPAC synthesis. Limnology and Oceanography 42, 405–418.

Laws, E.A., Falkowski, P.G., Smith, J., Walker, O., McCarthy, J.J., 2000a. Temperature effects on export production in the open ocean. Global Biogeochemical Cycles 14, 1231–1246.

Laws, E.A., Landry, M.R., Barber, R.T., Campbell, L., Dickson, M.-L., Marra, J., 2000b. Carbon cycling in primary production bottle incubations: inferences from grazing experiments and photosynthetic studies using ^{14}C and ^{18}O in the Arabian Sea. Deep-Sea Research II 47, 1339–1352.

Le Borgne, R., Gesbert, H., 1995. Campagne océanographique FLUPAC à bord du N. O. L'ATALANTE (23 septembre au 29 octobre 1994). Receuil de données. Tome 1: météo, courantologie, hydrologie, données de surface. ORSTOM-Nouméa, Archives, Sciences de la Mer océanographie 1, 340.

Le Borgne, R., Rodier, M., Le Bouteiller, A., Murray, J.W., 1999. Zonal variability of biological features and particle export flux in the Pacific equatorial upwelling between 165°E and 150°W (April–May 1996). Oceanologica Acta 22, 57–66.

Le Borgne, R., Barber, R.T., Delcroix, T., Inoue, H.Y., Mackey, D.J., Rodier, M., 2002. Pacific warm pool and divergence: temporal and zonal variations on the equator and their effects on the biological pump. Deep-Sea Research II 49, 2471–2512.

Le Bouteiller, A., Blanchot, J., Rodier, M., 1992. Size distribution patterns of phytoplankton in the western Pacific, towards a generalization for the tropical open ocean. Deep-Sea Research I 39, 805–823.

Loukos, H., Frost, B., Harrison, D.E., Murray, J.W., 1997. An ecosystem model with iron limitation of primary production in the equatorial Pacific at 140°W. Deep-Sea Research II 44, 2221–2249.

Martin, J.H., Coale, K.H., Johnson, K.S., Fitzwater, S.E., Gordon, R.M., Tanner, S.J., Hunter, C.N., Elrod, V.A., Nowiki, J.L., Coley, T.L., Barber, R.T., Lindley, S.T., Watson, A.J., Van Scoy, K., Law, C.S., Liddicoat, M.I., Ling, R., Stanton, T., Stockel, J., Collins, C., Anderson, A., Bidigare, R.R., Ondrusek, M.E., Latasa, M., Millero, F.J., Lee, K., Yao, W., Zhang, J.Z., Friederich, G., Sakamoto, C., Chavez, F.P., Buck, K., Kolber, Z., Greene, R., Falkowski, P.G., Chisholm, S.W., Hoge, F., Swift, R., Yungel, J., Turner, S., Nightingale, P., Hatton, A., Liss, P., Tindale, N.W., 1994. Testing the iron hypothesis in ecosystems of the equatorial Pacific Ocean. Nature 371, 123–129.

McCarthy, J.J., Garside, C., Nevins, J.L., Barber, R.T., 1996. New production along 140°W in the equatorial Pacific during and following the 1992 El Niño event. Deep-Sea Research II 43, 1065–1093.

McCarthy, J.J., Garside, C., Nevins, J.L., 1999. Nitrogen dynamics during the Arabian Sea Northeast Monsoon. Deep-Sea Research II 46, 1623–1664.

Morel, A., 1988. Optical modeling of the upper ocean in relation to its biogenous matter content (case I waters). Journal of Geophysical Research 93, 10749–10768.

Murray, J.W., Downs, J.N., Strom, S., Wei, C.-L., Jannasch, H.W., 1989. Nutrient assimilation, export production and 234Th scavenging in the eastern equatorial Pacific. Deep-Sea Research I 36, 1471–1489.

Murray, J.W., Barber, R.T., Roman, M.R., Bacon, M.P., Feely, R.A., 1994. Physical and biological controls on carbon cycling in the equatorial Pacific. Science 266, 58–65.

Navarette, C., 1998. Dynamique du phytoplancton en océan équitorial: mesures cytométriques and mesures isotopiques durant la campagne FluPac, en octobre 1994 dans la partie ouest du pacific. Doctoral dissertation, Université Paris VI, Paris.

Neter, J., Kutner, M.H., Nachtsheim, C.J., Wasserman, W., 1996. Applied Linear Regression Models. IRWIN/McGraw-Hill Professional Publishing, Chicago, p. 720.

Oudot, C., Montel, Y., 1988. A high sensitivity method for the determination of nanomolar concentrations of nitrate and nitrite in seawater with a Technicon AutoAnalyzer II. Marine Chemistry 24, 239–252.

Peña, M.A., Harrison, W.G., Lewis, M.R., 1992. New production in the central equatorial Pacific. Marine Ecology Progress Series 80, 265–274.

Platt, T., Harrison, W.G., 1985. Biogenic fluxes of carbon and oxygen in the ocean. Nature 318, 55–58.

Price, N.M., Ahner, B.A., Morel, F.M.M., 1994. The equatorial Pacific Ocean: grazer-controlled phytoplankton populations in an iron-limited ecosystem. Limnology and Oceanography 39, 520–534.

Probyn, T.A., Waldron, H.N., Searson, S., Owens, N.J.P., 1996. Diel variability in nitrogenous nutrient uptake at photic and sub-photic depths. Journal of Plankton Research 18, 2063–2079.

Raimbault, P., Slawyk, G., Boudjellal, B., Coatanoan, C., Conan, P., Coste, B., Garcia, N., Moutin, T., Pujo-Pay, M., 1999. Carbon and nitrogen uptake and export in the equatorial Pacific at 150°W: evidence of an efficient regenerated production cycle. Journal of Geophysical Research 104, 3341–3356.

Rayner, J.M.V., 1985. Linear relations in biomechanics: the statistics of scaling functions. Journal of the Zoological Society of London (A) 1985, 415–439.

Ricker, W.E., 1973. Linear regressions in fishery research. Journal of the Fisheries Research Board of Canada 30, 409–434.

Rodier, M.L, eBorgne, R., 1997. Export flux of particles at the equator in the western and central Pacific Ocean. Deep-Sea Research II 44, 2085–2113.

Sokal, R.R., Rohlf, F.J., 1995. Biometry: the Principles and Practice of Statistics in Biological Research. W. H. Freeman and Company, New York, p. 887.

Strickland, J., Parsons, T., 1972. A practical handbook of seawater analysis. Fisheries Research Board of Canada Bulletin 167, 310.

Villareal, T.A., Lipschultz, F., 1995. Internal nitrate concentrations in single cells of large phytoplankton from the Sargasso Sea. Journal of Phycology 31, 689–696.

Wheeler, P.A., 1994. Nutrient data for EqPac Times Series I and II. US JGOFS Web Page (http://www1.whoi.edu/jgofs.html).

Wheeler, P.A., 1995. New production data for EqPac Times Series I and II. US JGOFS Web Page (http://www1.whoi.edu/jgofs.html).

Wheeler, P.A., Kokkinakis, S.A., 1990. Ammonium recycling limits nitrate use in the oceanic subarctic Pacific. Limnology and Oceanography 35, 1267–1278.

Wilkerson, F.P., Dugdale, R.C., 1992. Measurements of nitrogen productivity in the equatorial Pacific. Journal of Geophysical Research 97, 669–679.